the possibility of direct binding of TRAF3 to TICAM-1 in human cells cannot be ruled out, a direct interaction could not be confirmed using yeast.

To confirm the associations identified in the yeast two-hybrid assay, immunoprecipitation (I.P.) analyses was performed and supported the interaction of TRAF2 and TICAM-1 (Fig. 1c and d). A similar coprecipitation was observed between TICAM-1 and either TRAF2 or TRAF6 (Fig. 1d and e). Subsequent i.p. analyses revealed that the C-terminal domains, which are highly conserved in TRAFs (Chung et al., 2002), of TRAF2 and TRAF6 bind TICAM-1 (Fig. 1d and e) and indicates that this region of TRAF1, 2, and 6 directly interacts with the N-terminal region of TICAM-1.

We next attempted to determine the precise region of TICAM-1 responsible for TRAF2 binding. The TRAF domain, a conserved region of approximately 180 aa, in the C-terminus of TRAF2 interacts with target molecules through the binding consensus sequence motifs (P/S/A/T)x(Q/E)E, PxQxxD, and PxQx(T/S) (Pullen et al., 1998; Lu et al., 2003). There are two such motifs in the N-terminal region of TICAM-1, represented by AYQE and PLQLS which are located at aa 117–120 and aa 333–337, respectively. To determine if TRAF2 requires these consensus sequences for interacting with TICAM-1, we constructed several truncated mutants of the TICAM-1 N-terminal region and analyzed their interaction with TRAF2 using the yeast two-hybrid system (Fig. 2a). Deletion of the first 200 aa in the N-terminus of the TICAM-1 S1 fragment (dN200) did not affect its binding ability to TRAF2, however, deletion of aa 200–359 (N200) did prevent its association. The dN300 fragment, containing only aa 300–359, was sufficient for binding TRAF2. Hence, while the consensus sequence PLQLS in TICAM-1 is critical for binding TRAF2, the AYQE sequence is dispensable for the association.

It has been reported that there are two pattern mutations in the PxQxS consensus sequence, represented by PxQxA and AxAxS (Lu et al., 2003). We therefore constructed both mutations in TICAM-1 dN300 (TICdN300 PQA and TICdN300 AAS) and examined the ability of these mutated proteins to bind TRAF2 in yeast. It was observed that either mutation of the PxQxS motif in TICAM-1 abolished the binding to TRAF2 (Fig. 2b). These data clearly demonstrate that TRAF2 directly binds the PLQLS sequence of TICAM-1.

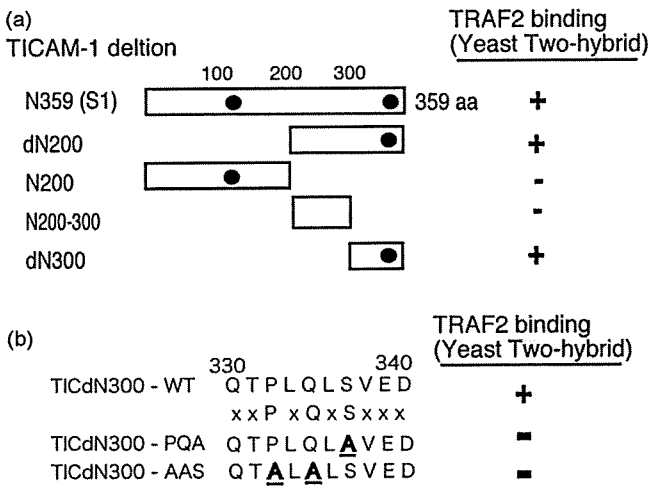

Fig. 2. Identification of the TRAF2-binding site in TICAM-1. (a) Scheme of TICAM-1 truncated mutants and location of the TRAF2 binding motif (black dot). TRAF2 in pGADT7 and each TICAM-1 construct in pGBKT7 were transformed into yeast. TRAF2 binding was assessed on SD-WLH plates as described in Fig. 1. (b) Specific consensus motif of TICAM-1 that directly binds to TRAF2. The predicted TRAF2 binding motif in TICAM-1 (TICdN300) was identified as the PxQxS sequence (300–359 aa). TICAM-1dN300 contained two alanine substitutions (TICdN300-PQA and TICdN300-AAS). These two alanine mutants were examined for their ability to bind TRAF2 by the yeast two-hybrid system. TRAF2 binding was assessed on SD-WLH plates.

We also confirmed a previous report which demonstrated that TRAF1 is a TICAM-1-interacting protein (Su et al., 2006). The TRAF-C domain of TRAF1 and the N + TIR domain of TICAM-1 were responsible for their interaction. In addition, it was shown that TRAF6 failed to couple with the E252A TICAM-1 mutant (data not shown) (Ye et al., 2002; Sato et al., 2003).

3.2. The function of TRAF2 binding to TICAM-1

As it has been reported that overexpression of TICAM-1 induces massive IFN-β promoter activation (Oshiumi et al., 2003a), the importance of TRAF binding in TICAM-1 signaling was examined by the ability of TICAM-1 mutant proteins to induce IFN-β promoter activation. As the C-terminal TICAM-1 region (containing the RHIM domain) recruits RIP1 and also activates NF-κB (Meylan et al., 2004), which is involved in IFN-β transcription and apoptosis signaling, we used a C-terminal-deleted TICAM-1 fragment, designated N + TIR (1–533 aa TICAM-1) (Funami et al., 2004) to eliminate the induced effects caused by C-terminal activity. Compared to the N + TIR fragment, which maintained wild-type levels of TICAM-1 IFN-β-inducing activity (Funami et al., 2004), the TICAM-1 PQA (S335A) mutation exhibited slightly reduced IFN-β promoter activation. However, the E252A mutation in TICAM-1, which is located in one of the TRAF6 binding motifs and facilitates TRAF6-TICAM-1 interaction (Jiang et al., 2004), largely impaired IFN-β promoter activation. Interestingly, a double mutation of E252A and PQA further reduced the activation compared to the E252A mutation alone (Fig. 3a). The reduction of IFN-β promoter activation was not caused by protein instability/degradation induced by the mutations, as the amount of N + TIR protein was nearly identical in the wild-type, PQA, E252A, and double-mutant TICAM-1 samples (Fig. 3a, inset). These data indicate that TRAF2 plays a role in TICAM-1-binding and activation of the IFN-β promoter, a conclusion which is supported by the effects of the TRAF6 site-mutation TICAM-1. Previous analysis concerning the role of TRAF6 in TICAM-1 signaling was performed with TRAF6- deficient mouse macrophages (Sato et al., 2003), and in those studies, TRAF2 was found to be intact. It is likely that TRAF6 was dispensable for TICAM-1 signaling due to the compensatory function of TRAF2 and suggests that TRAF2 expression levels would have affected the degree of activation of TICAM-1 signaling in *traf6* mutant cells.

We next examined IFN-β promoter activation and transcription of endogenous IFN-β mediated by full-length TICAM-1. In these experiments, a RHIM-mutated TICAM-1 (Meylan et al., 2004; Kaiser and Offermann, 2005) was used to circumvent apoptotic signaling by TICAM-1 and NF-κB activation through RIP1. A triple mutant of TICAM-1, consisting of E252A, PQA, and RHIM domain mutations, displayed a nearly complete abrogation of reporter activation (Fig. 3b) and induction of IFN-β transcription (Fig. 3c) compared to the wild-type and TICAM-1 RHIM-mutant. Taken together, these results indicate that the interaction of TRAF2 and TRAF6 with TICAM-1 is indispensable for IFN-β induction by overexpressed TICAM-1.

3.3. Transcription factors activated by TRAF2/6

IFN-β is transcribed by three transcription factors: NF-κB, IRF-3, and AP-1. To analyze which transcription factors are regulated by TRAF2/6 on TICAM-1 signaling, we performed a reporter gene assay for each of the three transcription factors using the TICAM-1 mutants (Fig. 4 and Supplementary data, Fig. S3). Although TRAF2 and TRAF6 are known to possess the ability to activate NF-κB, TICAM-1 with a mutated TRAF2-binding site (AAS and PQA) had increased activation of NF-κB compared to the control. The PQA/E252A double mutant displayed reduced NF-κB activation compared to the E252A mutant (Fig. 4b). Unexpectedly, the

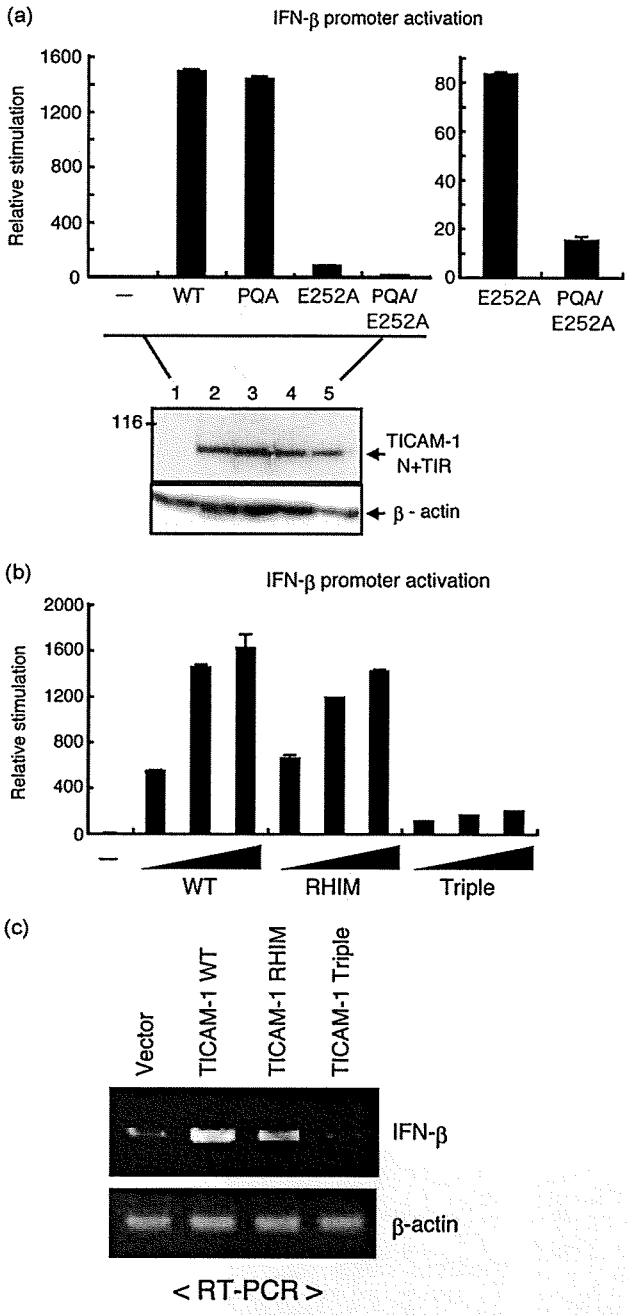

Fig. 3. TRAF2 and TRAF6 binding affect TICAM-1-mediated IFN-β induction. (a and b) HEK293 cells were transiently transfected with 10 ng (a) or 5, 25, 50 ng (b) of the indicated TICAM-1 mutant together with the p125-luc IFN-β promoter reporter plasmid (100 ng). Twenty-four hours after transfection, cells were harvested and the luciferase activities were measured. Data indicate the relative stimulation compared to vector transfection. Assays were performed three times in triplicate. One representative data set of three trials is shown. Bottom panel of (a) shows the expression level of each mutated TICAM-1. After the measurement of luciferase activity, each of the lysate samples were separated using SDS-PAGE, and the expression level of each mutant TICAM-1 was detected by anti-HA rabbit polyclonal antibody, and applied protein levels were detected by anti-β-actin mouse monoclonal antibody. (c) RAW 264.7 cells were transiently transfected with the indicated TICAM-1 constructs. Twenty-four hours after transfection, total RNA from the cells was isolated using RNeasy, and then reverse transcribed into cDNA. PCR was performed using primer sets for mouse IFN-β and β-actin, and PCR products were separated by gel electrophoresis on 1% agarose gels.

E252A/PQA double mutant also had impaired activation of IRF-3 (Fig. 4a) and perhaps to a lesser extent, AP-1 (Fig. 4c). For each transcription factor except for AP-1, a more profound suppression of transcriptional activation was observed in the E252A/PQA double mutant than in the E252A single mutant (Supplementary data, Fig. S3). These results indicate that the IFN-β-inducing signal is due to TICAM-1 oligomerization (Funami et al., 2008) which is regulated by the presence of TRAF2/6 proteins. Although endogenous TICAM-1 is usually present at low levels in non-stimulated cells and may still affect the reporter output, efficient inhibition of reporter activation by the double mutant was reproducible in repetitive experiments (Fig. 4 and Supplementary data, Fig. S3).

3.4. $PQ^{337}S$ and ^{252}E of TICAM-1 N+TIR are critical for TRAF2- and 6-recruitment

To clarify the participation of the single site of TICAM-1 N+TIR for TRAF2- and TRAF6-binding, confocal microscopy imaging analysis using labeled TRAF2, TRAF6, and TICAM-1 N+TIR was used (Fig. 5). While TRAF2 and TRAF6 merged with TICAM-1 N+TIR (upper panels) in overlayed images, under identical test conditions, both largely failed to overlap with the triple mutant (N+TIR/PQA/E252A) (lower panel). Using the TICAM-1 N+TIR mutants, it was confirmed that the PQA and E252A mutations resulted in non-overlapped images with TRAF2 and TRAF6, respectively (data not shown). Thus, there is a single site for TRAF2- and TRAF6-binding in N+TIR of TICAM-1 which is critical for IFN-β promoter activation and TICAM-1 N-terminal oligomerization.

Full-length TICAM-1 containing even single N-terminal mutations was still observed to merge with TRAF2 and TRAF6 in confocal images (data not shown), suggesting that TRAF2 and 6 bind to the C-terminal region of TICAM-1 in addition to the N-terminal sites. Under the same conditions, TRAF3 was recruited to TICAM-1 N+TIR as well as the triple mutant (Fig. 5, right panels). Since TICAM-1 has a TBK1-binding site apart from these TRAF-binding sites (Funami et al., 2007), TRAF3 may bind multiple regions of TICAM-1. Ultimately, the function of TICAM-1 may not be reflecting merely binding to TRAF3 as TICAM-1 overexpression induces TRAF2/6-mediated IFN-β promoter activation.

3.5. TICAM-1 ubiquitination induced by TRAF2

TRAF proteins are E3 ligases involved in the ubiquitination of proteins, an event which is often necessary for the activation of IRF-3. Although ubiquitination is prominent in RIG-I-mediated IRF-3 activation, TICAM-1 is also ubiquitinated during polyI:C stimulation or overexpression (Oshiumi et al., 2003a). We therefore tested whether TRAF2 ubiquitinates TICAM-1 in a similar manner to the activation of RIG-I by TRIM25, which leads to IRF-3 dimerization. When the N+TIR TICAM-1 fragment was co-expressed with TRAF2, the slow migration form of TICAM-1 was observed by SDS-PAGE and immunoblotting (Fig. 6a). To determine whether TICAM-1 was ubiquitinated, CFP-tagged TICAM-1, Flag-tagged TRAF2, and HA-tagged ubiquitin were first co-expressed in HEK293 cells, and lysates were immunoprecipitated with anti-GFP Ab to precipitate TICAM-1-CFP before being subjected to SDS-PAGE and i.p. analyses (Fig. 6b). After staining the blots with anti-HA Ab, high-molecular weight smeared HA-ubiquitin bands appeared when TICAM-1 was immunoprecipitated with anti-GFP Ab, while smeared ubiquitin bands were only slightly visible in the absence of TICAM-1 or TRAF2 (Fig. 6b).

To confirm the TRAF2-mediated polyubiquitination of TICAM-1, an *in vitro* ubiquitination assay was conducted using purified ubiquitin, E1, E2, TRAF2, and TICAM-1 proteins. The protein purity was determined by CBB staining of SDS-PAGE gels to be over 80% (Fig. 6c and data not shown). As revealed by immunoblotting using

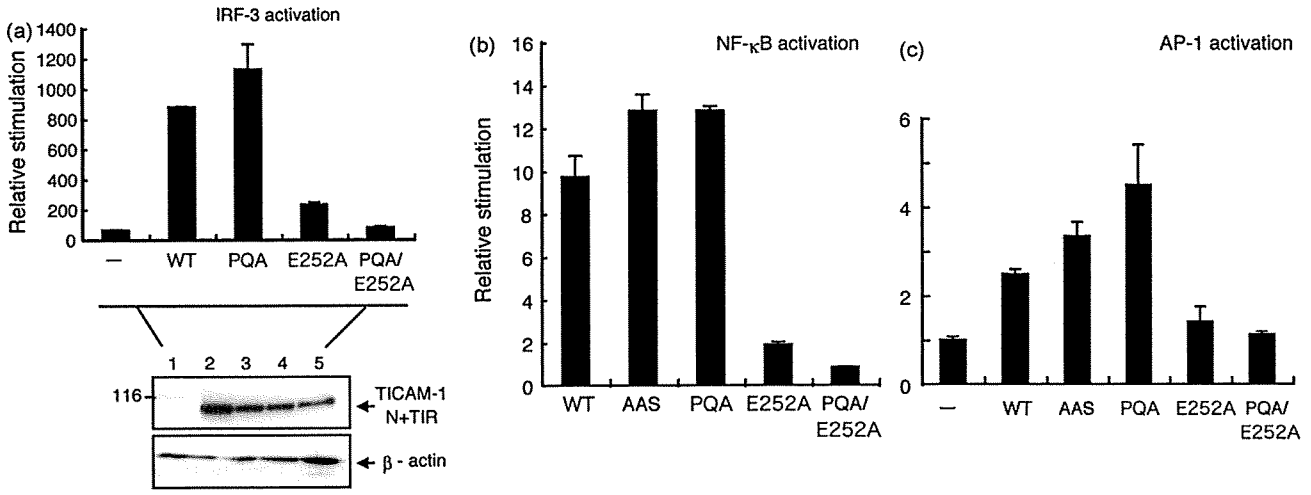

Fig. 4. Complete TRAF2/6 binding to TICAM-1 leads to activation of the transcription factors IRF-3, NF-κ B, and AP-1. (a–c) HEK293 cells were transiently transfected with 10 ng (a) or 200 ng (b and c) of the indicated TICAM-1 mutant plasmid together with p55 UASG-Luc reporter and either GAL4-IRF3 (a), NF-κB reporter (b) or AP-1 reporter (c) plasmid. Twenty-four hours after transfection, cells were harvested and the luciferase activities were measured. Data indicate the relative stimulation compared to empty vector transfection. Assays were performed three times in triplicate. The data are representative of three independent experiments. The bottom panel of (a) shows the expression level of TICAM-1 N+TIR. The method was identical to that described in Fig. 3.

anti-TICAM-1 Ab, *in vitro* TICAM-1 polyubiquitination was clearly observed only in the presence of the ubiquitin ligases and TRAF2 (Fig. 6d). Taken together, these data suggest that TRAF2 polyubiquitnates TICAM-1 to modify its function, although we could not determine whether TRAF2-mediated ubiquitination is specifically induced on TICAM-1.

Next, to determine which lysine residue of ubiquitin is used for polymerization, CFP-labeled TICAM-1 was transfected into HEK293 cells together with HA-labeled wild-type or mutant ubiquitin (K48R or K63R). After comparing the TICAM-1 ubiquitination profiles, K48R ubiquitin only marginally reduced polyubiquitination of TICAM-1 by TRAF2 (6.2 vs. 4.4) while ubiquitination by K63R was rarely observed on TICAM-1 by TRAF2 (6.2 vs. 1.4) in HEK cells (Fig. 6e). These data suggest that K63-linked polyubiquitination is dominant on TICAM-1 through the action of TRAF2 E3 ligase. The predominance of K63-linked polyubiquitination of TICAM-1 is consistent with the observation that TRAF2 and TRAF6 are important for sustaining (rather than impairing) TICAM-1 signaling. To confirm these results, TICAM-1 N+TIR with mutated TRAF2- and/or TRAF6-binding sites were used as substrates of ubiquitination in HEK293 cells. Although both the PQA and E252A mutants displayed reduced polyubiquitination, the modification was still observed at a higher frequency than the control (Fig. 6f). The PQA/E252A double mutation almost completely abrogated ubiquitination in parallel with the failure to recruit TRAF2/6 to TICAM-1 N+TIR (Fig. 6f). These data indicate that TRAF2 and TRAF6 have redundant functions with

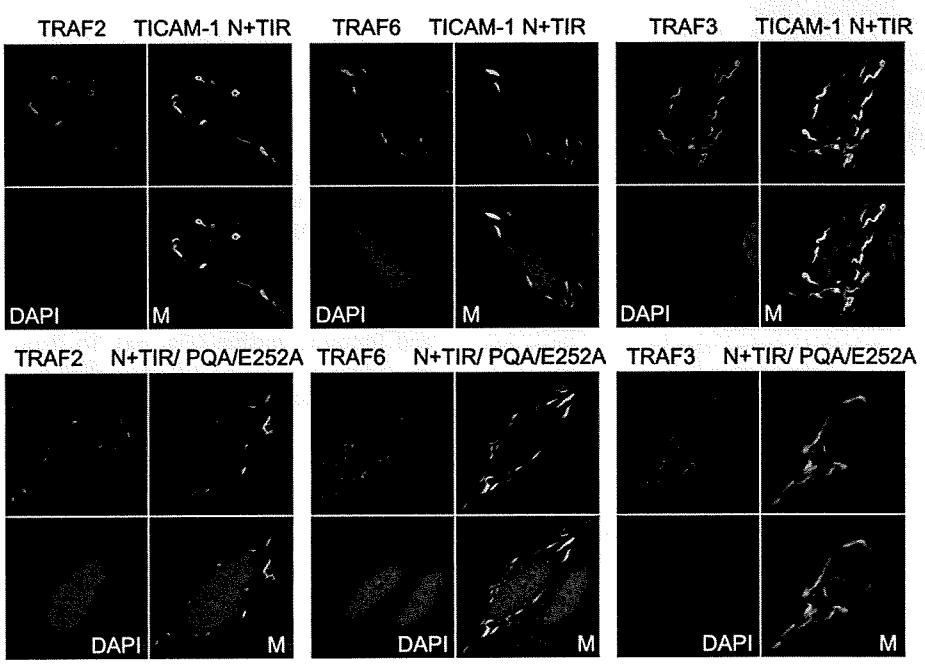

Fig. 5. Co-localization analysis of TICAM-1 N+TIR and TRAF proteins by confocal microscopy. HeLa cells were transfected with 30 ng of pECFP-N1 TICAM-1 and either 500 ng of pEF-BOS Flag-tagged TRAF2, TRAF6, or TRAF3. After 24 h, the cells were fixed, stained with anti-FLAG Ab, and then visualized with Alexa Fluor 568-conjugated secondary Ab. The same slide was also treated with DAPI for the staining of nuclei. M, Merging profile.

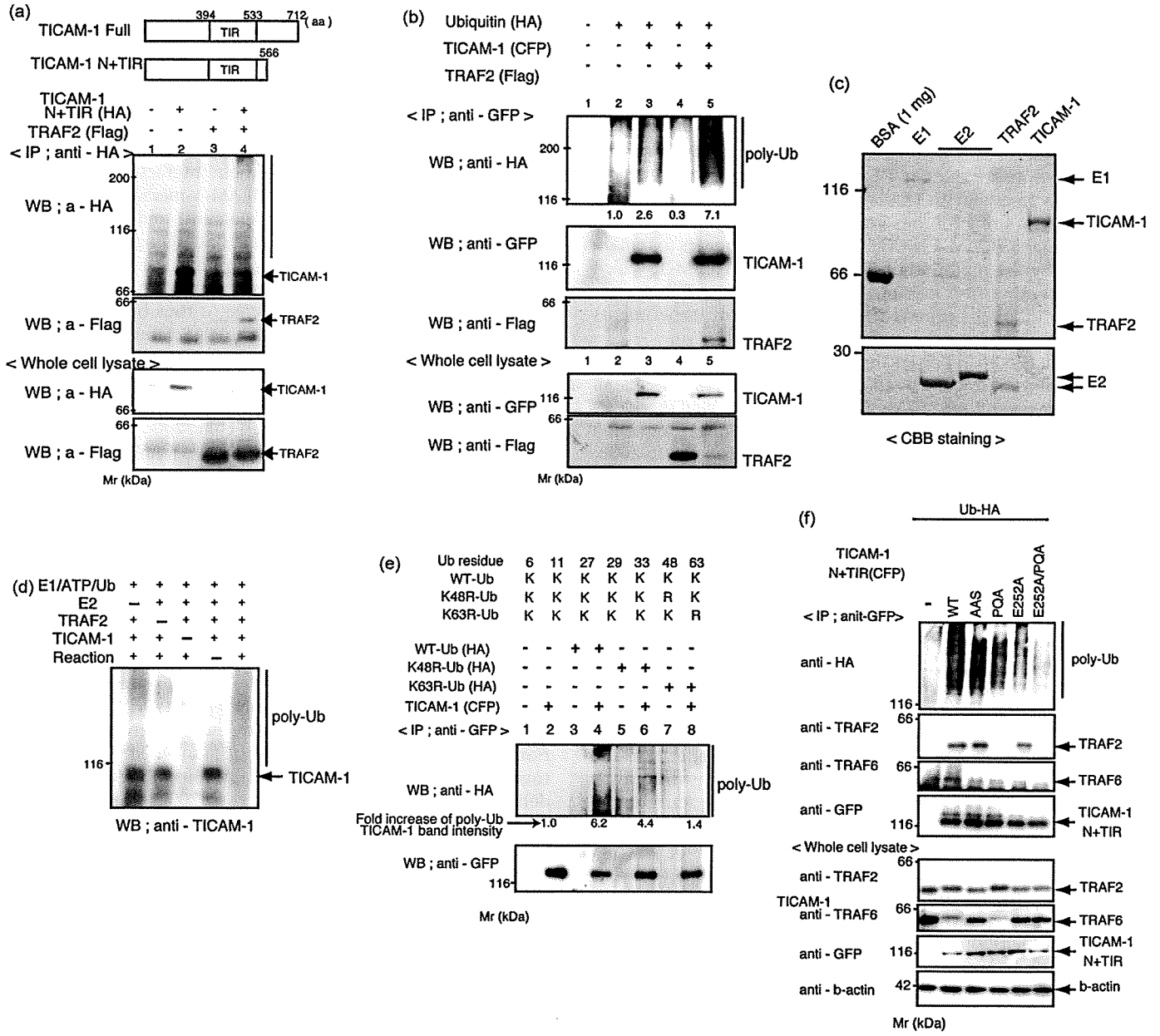

Fig. 6. TRAF2-mediated polyubiquitination of TICAM-1. (a) Interaction between TICAM-1, TICAM-1 N+TIR, and TRAF2. HEK293 cells were transfected with TICAM-1 N+TIR (HA) plasmid (100 ng) and TRAF2 (Flag) plasmid (2 μg) for expression of the indicated proteins. The total amount of DNA (4 μg/well) was kept constant by adding empty vector. Twenty-four hours after transfection, cells lysates were collected, proteins were immunoprecipitated, and the samples were analyzed by SDS-PAGE followed by immunoblotting. The upper two panels show immunoblots using the indicated Abs indicated, while the lower two panels show immunoblots of total cell lysates. (b) TICAM-1 polyubiquitination induced by TRAF2. HEK293 cells were transfected with plasmids for expression of TICAM-1 (CFP) (1 μg), TRAF2 (Flag) (1 μg) and/or ubiquitin (HA) (1 μg) as indicated. After 24 h, cells were lysed and proteins were immunoprecipitated with anti-GFP Ab. Ubiquitin (HA), TICAM-1 (GFP), and TRAF2 (FLAG) were probed with anti-HA, ant-GFP and anti-FLAG Abs, respectively, in the above blots. The protein content in each lysate is indicated at the bottom of the first immunoblot. The relative intensity of ubiquitination was measured using a densitometer. (c) Purity of the proteins used for *in vitro* ubiquitination. Purified proteins were resolved on SDS-PAGE gels (8%) and stained with Commassie brilliant blue to assess the protein concentration in each sample. (d) *In vitro* polyubiquitination of TICAM-1. The combinations of proteins used are indicated above the immuoblot. For the assay, 0.1 μg of E1, 0.5 μg of E2 (MMS2 0.25 μg, Ubc13 0.25 μg), 0.5 μg of TRAF2, 1 μg of ubiquitin and/or 1 μg of TICAM-1 proteins were incubated for 12 h at 30 °C in 20 μl of the reaction buffer (30 mM HEPES (pH7.5), 2 mM ATP, 5 mM $MgCl_2$, 0.2 mM DTT, 1 mM creatine phosphate, 10 U phosphocreatine kinase, and 10 mM phosphocreatine). The proteins were analyzed by SDS-PAGE, and immunoblotting was performed with anti-TICAM-1 Ab. The positions of TICAM-1 and ubiquitination are indicated to the right of the immunoblot. (e) K63-mediated polyubiquitination is dominant in TICAM-1. HEK293 cells were transfected with plasmids encoding TICAM-1 (CFP) (1 μg) and each ubiquitin (HA) plasmid (1 μg). The K48R and K63R ubiquitins were tested for site-specific ubiquitination by immunoprecipitation and blotting with anti-HA. TICAM-1 contents in the lysates are shown to the bottom. The fold increase in polyubiquitination (poly-Ub) intensities of the TICAM-1 band is indicated between the two immunoblots. (f) Effect of mutations of the TRAF2/6 binding site on the degree of TICAM-1 ubiquitination. HEK293 cells were transfected with plasmids encoding TICAM-1 N+TIR (CFP) (100 ng) and ubiquitin (HA) (1 μg). Cell lysates were analyzed by immunoprecipitation and blotting as indicated for each immunoblot. The positions of TRAF2, TRAF6, N+TIR, and β-actin (control) are indicated to the right of each immunoblot.

respect to protein modification by K63 ubiquitination, an observation which correlates with the ability of the N+TIR fragment to activate the IFN-β promoter and the IRF-3 and NF-κB transcription factors.

4. Discussion

Here we demonstrated that the N-terminal region of TICAM-1 recruits TRAF2 and TRAF6 through activation/oligomerization

and that both the TRAF6- and TRAF2-binding sites participate in TICAM-1-mediated IFN-β-induction. Although other TRAF2- and TRAF6-binding sites in the C-terminal region may further modify TICAM-1 function, we focused on the functional modulation of TICAM-1 N+TIR by TRAF2/6, and revealed that the TRAF2 site of TICAM-1 serves as a functional modulator in the absence of the TRAF6 site (Figs. 3 and 4 and Supplementary data, Fig. S3). Tantalized points are that (1) TICAM-1 polyubiquitination occurs essentially in parallel with TRAF2/6 function (Fig. 6), although the role of the ubiquitination has yet to be decisively revealed; (2) TRAF3 binding to TICAM-1 N+TIR unexpectedly appears to remain intact even by the mutation of TRAF2/6 sites in TICAM-1, which suggests that other sites mediate TRAF3-TICAM-1 N+TIR interaction (Fig. 5). Although beyond the scope of this study, experiments are underway to address these unsettled points.

Sato et al. (2003) reported that TRAF6 binds to TICAM-1 and plays an important role in NF-κB activation in TICAM-1-mediated signaling. However, *traf6−/−* knockout analysis showed that deletion of the TRAF6 gene does not impair cytokine production or transcription factor activation by TLR3 (Häcker et al., 2006; Oganesyan et al., 2006). Although this difference was attributed to preferential usage of TRAF subtypes by specific cell types (Gohda et al., 2004), these results suggest that TRAF6 is not the only TRAF that satisfy TLR3 signaling. We therefore constructed TICAM-1 mutants with disrupted TRAF6- or TRAF2-binding sites and demonstrated these sites are critical for mediating the function of TICAM-1, including IFN-β induction. To the best of our knowledge, this is the first study to provide evidence for the redundancy of TRAF2 and TRAF6 in TICAM-1-stimulated NF-κB and IRF-3 activation, and the possibility of K63-linked polyubiqutination for modifying the function of the TLR adaptor protein TICAM-1.

By mutational analysis, we found that disruption of the TRAF2-binding motif of TICAM-1 alone had very little effect on the activation of the IFN-β promoter. However, mutations in both the TRAF2- and TRAF6-binding sites resulted in reduced activation of the TICAM-1 pathway as well as TICAM-1 polyubiquitination. Synergistic activation of TRAF2 and TRAF6 may therefore increase the activation of the IFN-β promoter by the TICAM-1 pathway. Although the importance of TRAF2 has been demonstrated in TRAF2 KO mice, which are embryonic lethal due to apoptosis of hepatocytes, the definitive *in vivo* role of TRAF2 in this pathway is unknown. As previously suggested using *traf6*-disrupted cells, different results were obtained (Kawai and Akira, 2007; Sato et al., 2003; Gohda et al., 2004). Indeed, the expression levels of TRAF2 and TRAF6 differ depending on the cell type (Chung et al., 2002). In addition, our results further demonstrate the involvement of TRAF2 in the TICAM-1 pathway, although TRAF2 activity may be masked in cells with sufficient levels of TRAF6. The unsettled discrepancy in previous reports (Sato et al., 2003; Gohda et al., 2004) regarding the relative importance of TRAF6 in the TICAM-1 pathway may be explained by the joining of TRAF2 and TRAF6 in this pathway. A similar synergistic action of TRAF2 and TRAF6 was reported with CD40, which also recruits TRAF3 and induces the activation of multiple pathways (Davies et al., 2005). It can be concluded that in at least some cell lines and organs, TRAF2 may play a significant role in the TICAM-1 pathway, as in the case of CD40.

TRAF2 and TRAF6 are involved in many cytokine-producing pathways, such as IL-1R and RIG-I signaling. In the cytoplasmic virus recognition system, the adaptor of RIG-I/MDA5, termed IPS-1 (MAVS/Cardif/VISA), requires both TRAF2 and TRAF6 to activate NF-κB, but not for the activation of IRF-3 (Guo and Cheng, 2007). In contrast, TICAM-1 unequivocally employs both TRAF2 and TRAF6 for activation of both these transcription factors. TRAF2 and TRAF6 were also shown to act as E3 ligases for K63 ubiquitination of TICAM-1. It has been reported that TICAM-1 is an essential adaptor for the IFN-inducing pathway and has a unique role in driving predominant NK cell activation in dendritic cells (Akazawa et al., 2007). The functions of TICAM-1 may be dependent on the cell type and require the differential usage of TRAF2 and TRAF6 for signaling, as demonstrated in the IPS-1 pathway.

TRAF1 has been characterized as a TICAM-1-binding protein capable of negatively regulating TICAM-1 function (Su et al., 2006). The TRAF-C domain of TRAF1 and the TIR domain of TICAM-1 are responsible for their interaction, and overexpression of TRAF1 inhibits TLR3/TICAM-1-mediated activation of NF-κB, IFN-stimulated response element, and the IFN-β promoter. TRAF4 is also involved in the underlying mechanisms for silencing TLR-mediated signaling through the interaction with molecules harboring phagosome/endosome membrane (Takeshita et al., 2005). These TRAF family proteins thus bind TLRs to exert their inhibitory functions. As most TRAF family proteins bind TICAM-1, many modes of compensation might be involved in TICAM-1 ubiquitination and IFN-inducing signal modification.

Although TRAF3 is essential for TICAM-1 mediated IRF-3 activation (Häcker et al., 2006; Oganesyan et al., 2006), we were unable to detect the direct binding of TRAF3 to TICAM-1 in yeast cells. Confocal analysis did, however, suggest that TRAF3 is involved in the molecular complex containing TICAM-1, an observation which is consistent with previous reports (Häcker et al., 2006; Oganesyan et al., 2006). Although TRAF2 and TRAF3 compete for the same site in CD40 for their binding (Sanada et al., 2008), this determination was not feasible in the TICAM-1 molecule due to the fact that even in the N+TIR mutant, multiple TRAF3-binding sites are present, making it difficult to analyze TRAF2/6-mediated TRAF3 recruitment. Since TRAF3-binding to TICAM-1 is not completely abrogated by mutation of the TRAF2/6 sites in TICAM-1, it is most likely that TICAM-1 indirectly interacts with TRAF3 besides TRAF2/6. This TRAF3 recruitment may independently occur in addition to the event such that the TRAF2/6 associated with TICAM-1 in turn recruits TRAF3. TRAF3 can also couple with TAK1 and MAP to deliver signals to NEMO (IKKγ) (Leo et al., 2002) which suggests the reported IRF-3-activating kinase complex NAP1-IKKε/TBK1 (Sasai et al., 2005), consisting of a regulatory subunit and kinases, functions downstream of TRAF3 to form the TICAM-1 signalosome (Funami et al., 2007). This would explain why TBK1 and IKKε coprecipitate with TICAM-1 in polyI:C-activated cells (Oshiumi et al., 2010).

From the observed activation-mediated coprecipitation of TICAM-1 and IRF-3-activating kinases in this study, we speculate that TRAF proteins polyubiquitinate TICAM-1, as well as other assembled proteins, leading to the formation of a tight complex. Our protein-expression studies also suggest that TICAM-1 polyubiquitination and IRF-3 activation are correlated in HEK293 cells (Fig. 6). Furthermore, the involvement of A20 K63 deubiquitination enzyme in the regulation of TLR3 signaling have been reported (Wang et al., 2004; Saitoh et al., 2005). Although the specific details of time-dependence between TICAM-1 K63 ubiquitination and the induction of IFN-β remain to be investigated, we speculate that polyubiquitination of TICAM-1 by TRAF2 and TRAF6 is required for TICAM-1 to induce IRF-3 and NF-κB activation. This is supported by the observation that polyubiquitination of TICAM-1 was required for TRAF3-binding to TICAM-1 (Oganesyan et al., 2006). However, which E3 ligase is the best enhancer for TICAM-1 is a topic to be addressed in future experiments.

Acknowledgements

We thank the members of our laboratory for invaluable discussions. This work was supported in part by the Program of Founding Research Centers for Emerging and Reemerging Infectious Diseases, MEXT, Sapporo Biocluster "Bio-S", the Knowledge Cluster Initiative

of the MEXT, Grants-in-Aid from the Ministry of Education, Science, and Culture (Specified Project for Advanced Research) and the Ministry of Health, Labor, and Welfare of Japan, Mitsubishi Foundation, Mochida Foundation, NorthTec Foundation and Yakult Foundation. M.S was supported by a Research Fellowship of the Japan Society for the Promotion of Science. Dr. Greg Newton reviewed the manuscript.

Appendix A. Supplementary data

Supplementary data associated with this article can be found, in the online version, at doi:10.1016/j.molimm.2009.12.002.

References

Akazawa, T., Ebihara, T., Okuno, M., Okuda, Y., Shingai, M., Tsujimura, K., Takahashi, T., Ikawa, M., Okabe, M., Inoue, N., Okamoto-Tanaka, M., Ishizaki, H., Miyoshi, J., Matsumoto, M., Seya, T., 2007. Antitumor NK activation induced by the Toll-like receptor 3-TICAM-1 (TRIF) pathway in myeloid dendritic cells. Proc. Natl. Acad. Sci. U.S.A. 104, 252–257.

Chung, J.Y., Park, Y.C., Ye, H., Wu, H., 2002. All TRAFs are not created equal: common and distinct molecular mechanisms of TRAF-mediated signal transduction. J. Cell. Sci. 115, 679–688 (Review).

Davies, C.C., Mak, T.W., Young, L.S., Eliopoulos, A.G., 2005. TRAF6 is required for TRAF2-dependent CD40 signal transduction in nonhemopoietic cells. Mol. Cell. Biol. 25, 9806–9819.

Ermolaeva, M.A., Michallet, M.C., Papadopoulou, N., Utermöhlen, O., Kranidioti, K., Kollias, G., Tschopp, J., Pasparakis, M., 2008. Function of TRADD in tumor necrosis factor receptor 1 signaling and in TRIF-dependent inflammatory responses. Nat. Immunol. 9, 1037–1046.

Funami, K., Matsumoto, M., Oshiumi, H., Akazawa, T., Yamamoto, A., Seya, T., 2004. The cytoplasmic 'linker region' in Toll-like receptor 3 controls receptor localization and signaling. Int. Immunol. 16, 1143–1154.

Funami, K., Sasai, M., Ohba, Y., Oshiumi, H., Seya, T., Matsumoto, M., 2007. Spatiotemporal mobilization of Toll/1L-1 receptor domain-containing adaptor molecule-1 in response to dsRNA. J. Immunol. 179, 6867–6872.

Funami, K., Sasai, M., Oshiumi, H., Seya, T., Matsumoto, M., 2008. Homo-oligomerization is essential for Toll/interleukin-1 receptor domain-containing adaptor molecule-1-mediated NF-kappaB and interferon regulatory factor-3 activation. J. Biol. Chem. 283, 18283–18291.

Gohda, J., Matsumura, T., Inoue, J., 2004. Cutting edge: TNFR-associated factor (TRAF) 6 is essential for MyD88-dependent pathway but not Toll/IL-1 receptor domain-containing adaptor-inducing IFN-beta (TRIF)-dependent pathway in TLR signaling. J. Immunol. 173, 2913–2917.

Guo, B., Cheng, G., 2007. Modulation of the interferon antiviral response by the TBK1/IKKi adaptor protein TANK. J. Biol. Chem. 282, 11817–11826.

Häcker, H., Vabulas, R.M., Takeuchi, O., Hoshino, K., Akira, S., Wagner, H., 2000. Immune cell activation by bacterial CpG-DNA through myeloid differentiation marker 88 and tumor necrosis factor receptor-associated factor (TRAF)6. J. Exp. Med. 192, 595–600.

Häcker, H., Redecke, V., Blagoev, B., Kratchmarova, I., Hsu, L.C., Wang, G.G., Kamps, M.P., Raz, E., Wagner, H., Häcker, G., Mann, M., Karin, M., 2006. Specificity in Toll-like receptor signalling through distinct effector functions of TRAF3 and TRAF6. Nature 439, 204–207.

Hirano, A., Kurita-Taniguchi, M., Katayama, Y., Matsumoto, M., Wong, T.C., Seya, T., 2002. Ligation of human CD46 with purified complement C3b or F(ab')(2) of monoclonal antibodies enhances isoform-specific interferon gamma-dependent nitric oxide production in macrophages. J. Biochem. 132, 83–91.

Ishida, T., Mizushima, S., Azuma, S., Kobayashi, N., Tojo, T., Suzuki, K., Aizawa, S., Watanabe, T., Mosialos, G., Kieff, E., Yamamoto, T., Inoue, J., 1996. Identification of TRAF6, a novel tumor necrosis factor receptor-associated factor protein that mediates signaling from an amino-terminal domain of the CD40 cytoplasmic region. J. Biol. Chem. 271, 28745–28748.

Jiang, Z., Mak, T.W., Sen, G., Li, X., 2004. Toll-like receptor 3-mediated activation of NF-kappaB and IRF3 diverges at Toll-IL-1 receptor domain-containing adapter inducing IFN-beta. Proc. Natl. Acad. Sci. U.S.A. 101, 3533–3538.

Kaiser, W.J., Offermann, M.K., 2005. Apoptosis induced by the Toll-like receptor adaptor TRIF is dependent on its receptor interacting protein homotypic interaction motif. J. Immunol. 174, 4942–4952.

Kawai, T., Akira, S., 2007. Signaling to NF-kappaB by Toll-like receptors. Trends Mol. Med. 13, 460–469 (Review).

Leo, A., Wienands, J., Baier, G., Horejsi, V., Schraven, B., 2002. Adapters in lymphocyte signaling. J. Clin. Invest. 109, 301–309 (Review).

Lu, L.F., Cook, W.J., Lin, L.L., Noelle, R.J., 2003. CD40 signaling through a newly identified tumor necrosis factor receptor-associated factor 2 (TRAF2) binding site. J. Biol. Chem. 278, 45414–45418.

Mansell, A., Brint, E., Gould, J.A., O'Neill, L.A., Hertzog, P.J., 2004. Mal interacts with tumor necrosis factor receptor-associated factor (TRAF)-6 to mediate NF-kappaB activation by Toll-like receptor (TLR)-2 and TLR4. J. Biol. Chem. 279, 37227–37230.

McKenna, S., Spyracopoulos, L., Moraes, T., Pastushok, L., Ptak, C., Xiao, W., Ellison, M.J., 2001. Noncovalent interaction between ubiquitin and the human DNA repair protein Mms2 is required for Ubc13-mediated polyubiquitination. J. Biol. Chem. 276, 40120–40126.

Meylan, E., Burns, K., Hofmann, K., Blancheteau, V., Martinon, F., Kelliher, M., Tschopp, J., 2004. RIP1 is an essential mediator of Toll-like receptor 3-induced NF-kappa B activation. Nat. Immunol. 5, 503–507.

Oganesyan, G., Saha, S.K., Guo, B., He, J.Q., Shahangian, A., Zarnegar, B., Perry, A., Cheng, G., 2006. Critical role of TRAF3 in the Toll-like receptor-dependent and -independent antiviral response. Nature 439, 208–211.

Oshiumi, H., Matsumoto, M., Funami, K., Akazawa, T., Seya, T., 2003a. TICAM-1, an adaptor molecule that participates in Toll-like receptor 3-mediated interferon-beta induction. Nat. Immunol. 4, 161–167.

Oshiumi, H., Sasai, M., Shida, K., Fujita, T., Matsumoto, M., Seya, T., 2003b. TIR-containing adapter molecule (TICAM)-2, a bridging adapter recruiting to Toll-like receptor 4 TICAM-1 that induces interferon-beta. J. Biol. Chem. 278, 49751–49762.

Oshiumi, H., Matsumoto, M., Hatakeyama, S., Seya, T., 2009a. Riplet/RNF135, a RING-finger protein, ubiquitinates RIG-I to promote interferon-b induction during the early phase of viral infection. J. Biol. Chem. 284, 807–817.

Oshiumi, H., Sakai, K., Matsumoto, M., Seya, T. 2010. DEAD/H BOX 3 (DDX3) helicase binds the RIG-I adaptor IPS-1 to up-regulate IFN-β inducing potential. Eur. J. Immunol (in press).

Pullen, S.S., Miller, H.G., Everdeen, D.S., Dang, T.T., Crute, J.J., Kehry, M.R., 1998. CD40-tumor necrosis factor receptor-associated factor (TRAF) interactions: regulation of CD40 signaling through multiple TRAF binding sites and TRAF hetero-oligomerization. Biochemistry 37, 11836–11845.

Saitoh, T., Yamamoto, M., Miyagishi, M., Taira, K., Nakanishi, M., Fujita, T., Akira, S., Yamamoto, N., Yamaoka, S., 2005. A20 is a negative regulator of IFN regulatory factor 3 signaling. J. Immunol. 174, 1507–1512.

Sanada, T., Takaesu, G., Mashima, R., Yoshida, R., Kobayashi, T., Yoshimura, A., 2008. FLN29 deficiency reveals its negative regulatory role in the Toll-like receptor (TLR) and retinoic acid-inducible gene I (RIG-I)-like helicase signaling pathway. J. Biol. Chem. 283, 33858–33864.

Sasai, M., Oshiumi, H., Matsumoto, M., Inoue, N., Fujita, F., Nakanishi, M., Seya, T., 2005. Cutting edge: NF-kappaB-activating kinase-associated protein 1 participates in TLR3/Toll-IL-1 homology domain-containing adapter molecule-1-mediated IFN regulatory factor 3 activation. J. Immunol. 174, 27–30.

Sato, S., Sugiyama, M., Yamamoto, M., Watanabe, Y., Kawai, T., Takeda, K., Akira, S., 2003. Toll/IL-1 receptor domain-containing adaptor inducing IFN-beta (TRIF) associates with TNF receptor-associated factor 6 and TANK-binding kinase 1, and activates two distinct transcription factors, NF-kappa B and IFN-regulatory factor-3, in the Toll-like receptor signaling. J. Immunol. 171, 4304–4310.

Shieh, H.L., Chen, Y., Brown, C.R., Chiang, H.L., 2001. Biochemical analysis of fructose-1,6-bisphosphatase import into vacuole import and degradation vesicles reveals a role for UBC1 in vesicle biogenesis. J. Biol. Chem. 276, 10398–10406.

Su, X., Li, S., Meng, M., Qian, W., Xie, W., Chen, D., Zhai, Z., Shu, H.B., 2006. TNF receptor-associated factor-1 (TRAF1) negatively regulates Toll/IL-1 receptor domain-containing adaptor inducing IFN-beta (TRIF)-mediated signaling. Eur. J. Immunol. 36, 199–206.

Takeshita, F., Ishii, K.J., Kobiyama, K., Kojima, Y., Coban, C., Sasaki, S., Ishii, N., Klinman, D.M., Okuda, K., Akira, S., Suzuki, K., 2005. TRAF4 acts as a silencer in TLR-mediated signaling through the association with TRAF6 and TRIF. Eur. J. Immunol. 35, 2477–2485.

Wang, Y.Y., Li, L., Han, K.J., Zhai, Z., Shu, H.B., 2004. A20 is a potent inhibitor of TLR3- and Sendai virus-induced activation of NF-kappaB and ISRE and IFN-beta promoter. FEBS Lett. 576, 86–90.

Ye, H., Arron, J.R., Lamothe, B., Cirilli, M., Kobayashi, T., Shevde, N.K., Segal, D., Dzivenu, O.K., Vologodskaia, M., Yim, M., Du, K., Singh, S., Pike, J.W., Darnay, B.G., Choi, Y., Wu, H., 2002. Distinct molecular mechanism for initiating TRAF6 signalling. Nature 418, 443–447.

Yoneyama, M., Suhara, W., Fukuhara, Y., Fukuda, M., Nishida, E., Fujita, T., 1998. Direct triggering of the type I interferon system by virus infection: activation of a transcription factor complex containing IRF-3 and CBP/p300. EMBO J. 17, 1087–1095.

European Journal of Immunology

Oligomerized TICAM-1 (TRIF) in the cytoplasm recruits nuclear BS69 to enhance NF-κB activation and type I IFN induction

Hiromi Takaki, Hiroyuki Oshiumi*, Miwa Sasai, Takahiro Kawanishi, Misako Matsumoto and Tsukasa Seya*

Department of Microbiology and Immunology, Graduate School of Medicine, Hokkaido University, Kita-ku, Sapporo, Japan

Although adenovirus 5 E1A-binding protein (BS69) is a nuclear protein acting as a transcriptional repressor, we found by an yeast two-hybrid and human cell immunoprecipitation another cytoplasmic function for this protein. BS69 bound Toll-interleukin 1 receptor domain (TIR)-containing adaptor molecule-1 (TICAM-1) (also named TRIF), an adaptor protein that couples with TLR3 around the endosome. BS69 translocated from the nucleus to the cytoplasm when cells were stimulated with dsRNA or transfected with TICAM-1. Confocal analysis of cells with over-expressed TICAM-1 or those stimulated with dsRNA revealed the characteristic "TICAM-1 speckle", which reflects signalosome formation necessary for the activation of NF-κB and IFN-regulatory factor (IRF)-3. BS69 was involved in the TICAM-1 complex, and the activation of NF-κB/IRF-3 followed by cytokine production was augmented in the presence of BS69 overexpression. Knockdown of endogenous BS69 resulted in a decrease of IFN-β induction, suggesting that BS69 is a positive regulator for the TLR3-TICAM-1 pathway. These results, together with a recent report showing the negative regulatory properties of BS69 in NF-κB activation by EBV-derived latent membrane protein 1, suggest that BS69 harbors dual modes of cytoplasmic NF-κB regulation, positively in the TICAM-1 pathway and negatively in the latent membrane protein 1 pathway.

Key words: BS69 · IFN-β · NF-κB · TICAM-1/TRIF · TLR3

Supporting Information available online

Introduction

Toll-interleukin 1 receptor domain (TIR)-containing adaptor molecule-1 (TICAM-1) acts as an adaptor for TLR3 and activates both the IFN-regulatory factor (IRF)-3 and the IFN-β promoter [1]. TLR3 is localized to the endosome in immature myeloid dendritic cells (mDC) and resting macrophages [2]. Recent imaging analyses revealed that TICAM-1 merges with endosomal TLR3 within 20 min in response to dsRNA stimuli, and after 60 min translocates to form speckles in the cytoplasm which represent the TICAM-1 signalosome [3]. NAP1 and RIP1 are recruited to the TICAM-1 complex, both of which are known to be important factors for activating downstream elements of the TICAM-1 pathway [3, 4]. The forced expression of TICAM-1 leads to the formation of multimers in the signalosome complex [4]. To elucidate what molecules constitute the TICAM-1 complex, we screened TICAM-1-binding proteins by

Correspondence: Dr. Tsukasa Seya
e-mail: seya-tu@pop.med.hokudai.ac.jp

*These authors contributed equally to this work.

an yeast two-hybrid assay. We identified adenovirus 5 E1A-binding protein (BS69) as a member of the TICAM-1 signalosome, in addition to the TRAF family proteins previously noted [1].

BS69, a multidomain cellular protein containing PHD, Bromo, PWWP and MYND domains [5], was originally identified as an adenovirus E1A-binding protein that inhibits the transactivation function of E1A [6, 7]. The C-terminal MYND domain of BS69 was shown to bind to the PxLxP motif existing on E1A, EBV-encoded EBNA2 and a Myc-related cellular protein MGA [8]. Although BS69 is unequivocally a nuclear protein, it has been shown that BS69 interacts with EBV-encoded latent membrane protein 1 (LMP1) in the cytoplasm through its MYND domain and acts as a scaffold protein in the LMP1-mediated JNK pathway by interacting with TRAF6 [9]. Furthermore, a recent report speculated that nuclear BS69 colocalizes with LMP1 in the cytoplasm proximal to the nucleus [10]. The stimulus which induces BS69 protein trafficking, however, remains undetermined.

In this study, we identified BS69 as a TICAM-1-binding protein and demonstrated that the TLR3 agonist polyI:C facilitates the BS69 nucleus-to-cytoplasm trafficking. This property of BS69 further highlights the function of this protein in the cytoplasm: BS69 is involved in the TICAM-1 complex and participates in TICAM-1-mediated IRF-3 and NF-κB activation. Here, we clarified a trigger of BS69 movement and the function of BS69 in the TICAM-1 pathway.

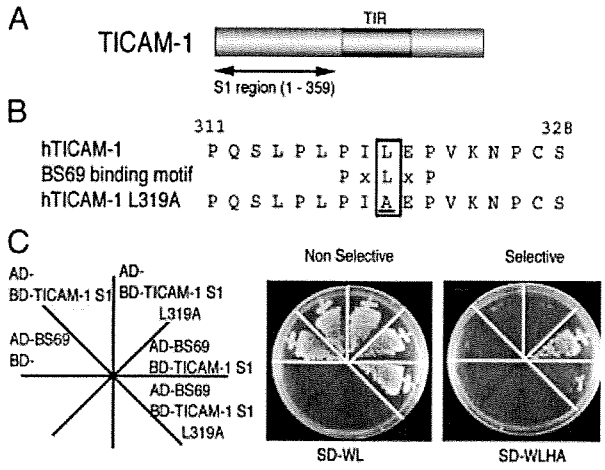

Figure 1. Yeast two-hybrid screening for the collection of TICAM-1-binding proteins. (A) The schema of human TICAM-1 protein. The S1 region (1–359 aa) of TICAM-1 was inserted into the pGBKT7 (bait) vector. From a total of 2.2 billion genes, six genes were obtained which encode for gene products capable of binding to the TICAM-1-S1 region. (B) Sequence alignment of human TICAM-1 and the BS69-binding motif (PxLxP). A point mutation (L319A) was introduced into the PxLxP motif. (C) Interaction between TICAM-1 S1 and BS69 in the yeast two-hybrid system. A strong association was observed between TICAM-1 S1 and BS69 (SD-WLHA plate), whereas the TICAM-1 S1 L319A-BS69 association was barely observable in the SD-WLHA plate.

Results

Yeast two-hybrid screening for collection of TICAM-1-binding proteins

TICAM-1 is a 712 aa protein (Fig. 1A). Since high background expression disturbed screening with the full-length protein, two segments consisting of the N-terminal S1 (1–359 aa) and C-terminal S2 (368-712 aa) regions were separately expressed in yeast (Fig. 1A). No growth was observed in yeast expressing solely S1 (Fig. 1C). The S1 and S2 fragments were ligated into pGBD-C1 and pGBKT7, respectively, to act as bait plasmids. The yeast cells containing bait plasmids were cultured on SD medium lacking Trp, Leu and His, while those cells harboring prey plasmids containing a human lung cDNA library were cultured on SD medium without Trp, Leu, His and Ade. Positive colonies were harvested and retested in the same growth medium (Fig. 1C). Six genes were finally obtained which encoded for gene products responsible for the S1 binding (data not shown). BS69 as well as TRAF-1, TRAF-2 and TRAF-6 were identified as TICAM-1-binding molecules. A reported BS69-binding motif, PxLxP, was identified in the 317–321 aa portion of TICAM-1 (Fig. 1B).

BS69 as a TICAM-1 N-terminal-binding protein

The direct binding of BS69 to the N-terminal of TICAM-1 was confirmed by retesting in yeast. We found the PxLxP motif at 317–321 aa in the TICAM-1 S1 fragment was crucial for BS69 binding, since a TICAM-1 S1 mutant (mt) containing a single point mutation (L319A) resulting in PxAxP, failed to bind BS69 (Fig. 1C). Next, plasmids with the BS69 cDNA and TICAM-1 cDNA were transfected into HEK293 cells and immunoprecipitation was performed. As observed in the yeast cells, WT TICAM-1 coprecipitated with BS69 (Fig. 2A). When the PxLxP motif in the N-terminal region of TICAM-1 was mutated to PxAxP, no BS69 binding was observed (data not shown). Hence, the mt lost the ability to bind BS69 in human cells as well as yeast, indicating that BS69 directly binds the PxLxP motif in the TICAM-1 molecule.

The interaction between TICAM-1 and BS69 was further examined in human cells by molecular imaging. When WT TICAM-1 was co-expressed with BS69 in HeLa cells, the majority of cells showed typical speckle-like TICAM-1 expression (Fig. 2B). This is consistent with a previous report [4], although ~30% of the cells displayed a diffuse expression profile of TICAM-1 (Fig. 2C). BS69 was exclusively stained in the nucleus in cells with diffuse TICAM-1 expression. Surprisingly, in cells with speckled TICAM-1, the cytoplasmic TICAM-1 merged with BS69 by FLAG tag staining. The results indicate that BS69 translocates from the nucleus to the cytoplasm by TICAM-1 over-expression and binds speckled TICAM-1 in the cytoplasm.

The TICAM-1 RHIM mt is efficiently expressed in cells without the induction of apoptosis [3], whereas TICAM-1 N+TIR P434H lacks the two sites essential for self-oligomerization [4]. We found that BS69 recruitment by TICAM-1 occurs in parallel with TICAM-1 oligomerization (speckle formation), since the RHIM mt

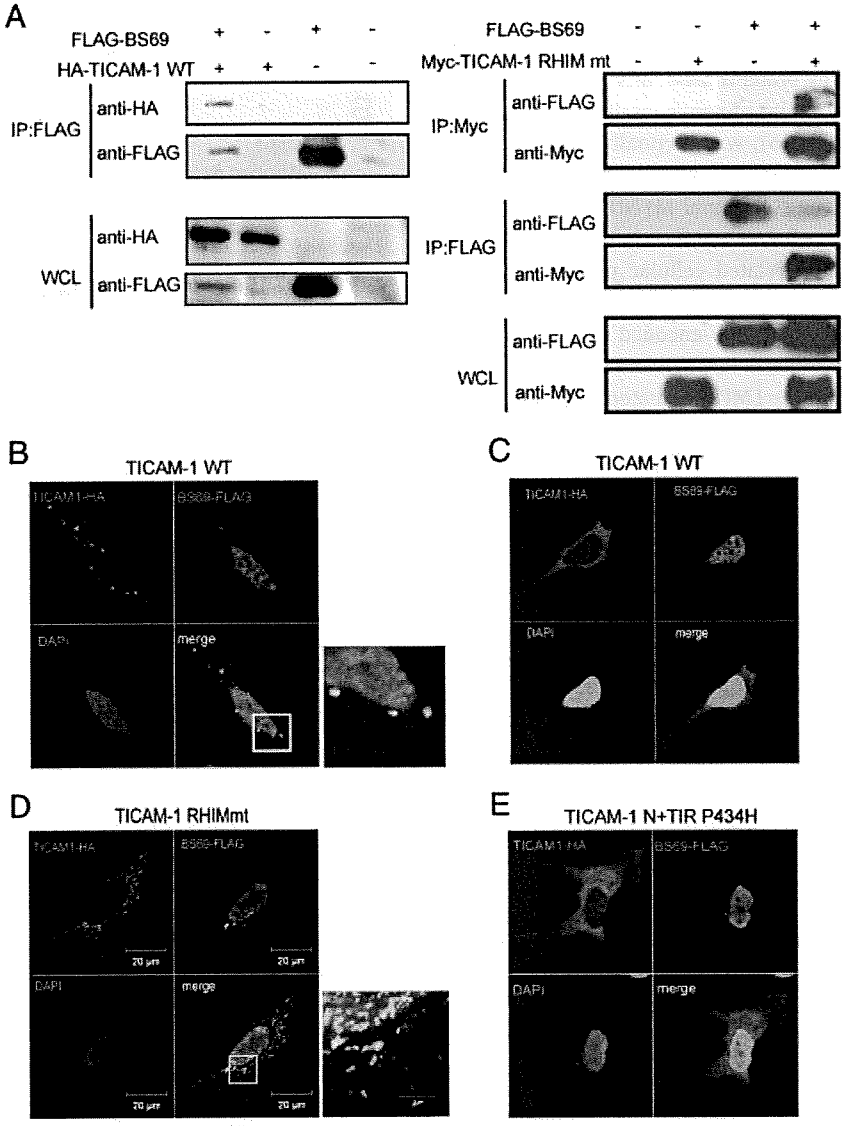

Figure 2. BS69 co-localizes with activated TICAM-1. (A) *Left panel*, HEK 293T cells were transfected with pEF-BOS HA-TICAM-1 WT and pEF-BOS FLAG-BS69. After 24 h, the cells were lysed, immunoprecipitated with anti-FLAG Ab and immunoblotted with anti-HA or anti-FLAG Ab. An aliquot of each whole cell lysate (WCL) was immunoblotted with either anti-HA or anti-FLAG Ab. A typical speckle pattern of TICAM-1 was observed. *Right panel*, HEK 293T cells were transfected with pEF-BOS Myc-TICAM-1 RHIM mt and pEF-BOS FLAG BS69. After 24 h, the cells were lysed, immunoprecipitated with anti-FLAG or anti-Myc Ab and immunoblotted with anti-Myc or anti-FLAG Ab. An aliquot of each whole cell lysate (WCL) was immunoblotted with either anti-Myc or anti-FLAG Ab. (B and C) HeLa cells were transfected with 1 ng of pEF-BOS HA-human TICAM-1 WT and 400 ng of pEF-BOS FLAG-human BS69. After 24 h, the cells were fixed and stained with anti-HA and anti-FLAG Ab, and visualized with either Alexa Fluor 488- or Alexa Fluor 594-conjugated secondary Ab. The same slide was also treated with DAPI for the staining of nuclei. (B) The transfected HeLa cell with activated TICAM-1, whereas (C) shows a cell with inactive TICAM-1. (D) TICAM-1 RHIM mt was transfected into HeLa cells instead of TICAM-1 WT. (E) TICAM-1 N+TIR P434H was transfected into HeLa instead of TICAM-1 WT. The transfection and staining conditions were identical to those in (B). An enlarged scale of the area within the white square in the merged image in (B) and (D) is shown to the right of the image.

recruited BS69 (Fig. 2D), whereas TICAM-1 N+TIR P434H failed to recruit BS69 in the cytoplasm (Fig. 2E).

Translocation of BS69 in response to TICAM-1 signaling

To observe the nucleus-to-cytoplasm shuttling of BS69, HEK293T cells were transfected with the FLAG-BS69 and HA-TICAM-1 plasmids, and 24 h later the cells were solubilized to separate the nuclei and cytoplasm. Each fraction was further solubilized and immunoprecipitated with anti-FLAG and anti-HA Ab (Fig. 3A). The cytoplasmic fraction did not contain any detectable lamin A, suggesting that nuclear contamination in the cytoplasmic fraction was negligible (Fig. 3A center panel). TICAM-1 overexpression clearly allowed some BS69 to move to the cytoplasm (Fig. 3A). The dynamics of BS69 translocation in response to TICAM-1 stimulation was then examined using polyI:C as a TLR3/TICAM-1 stimulator [1]. Cytoplasmic BS69 was detected 3 h after

polyI:C stimulation in both HeLa (Fig. 3B) and HEK293T cells (Fig. 3C). Imaging analysis using the polyI:C-stimulated cells indicated that cytoplasmic speckle formation of BS69 and TICAM-1 also appeared 3 h after polyI:C stimulation (Fig. 3D). PolyI:C stimulation barely altered the BS69 mRNA levels (data not shown). Hence, BS69 moves from the nucleus to the cytoplasm in association with the activation and oligomerization of TICAM-1.

BS69 is a positive regulator of the TICAM-1 pathway

We next examined if the TICAM-1 signal was enhanced by transfected BS69. NF-κB activation was up-regulated by the over-expression of BS69 (Fig. 4A). PolyI:C-dependent induction of IFN-β luciferase was also enhanced by the transfection and expression of BS69 in HEK293T and HeLa cells (Fig. 4B and C). IFN-β mRNA levels

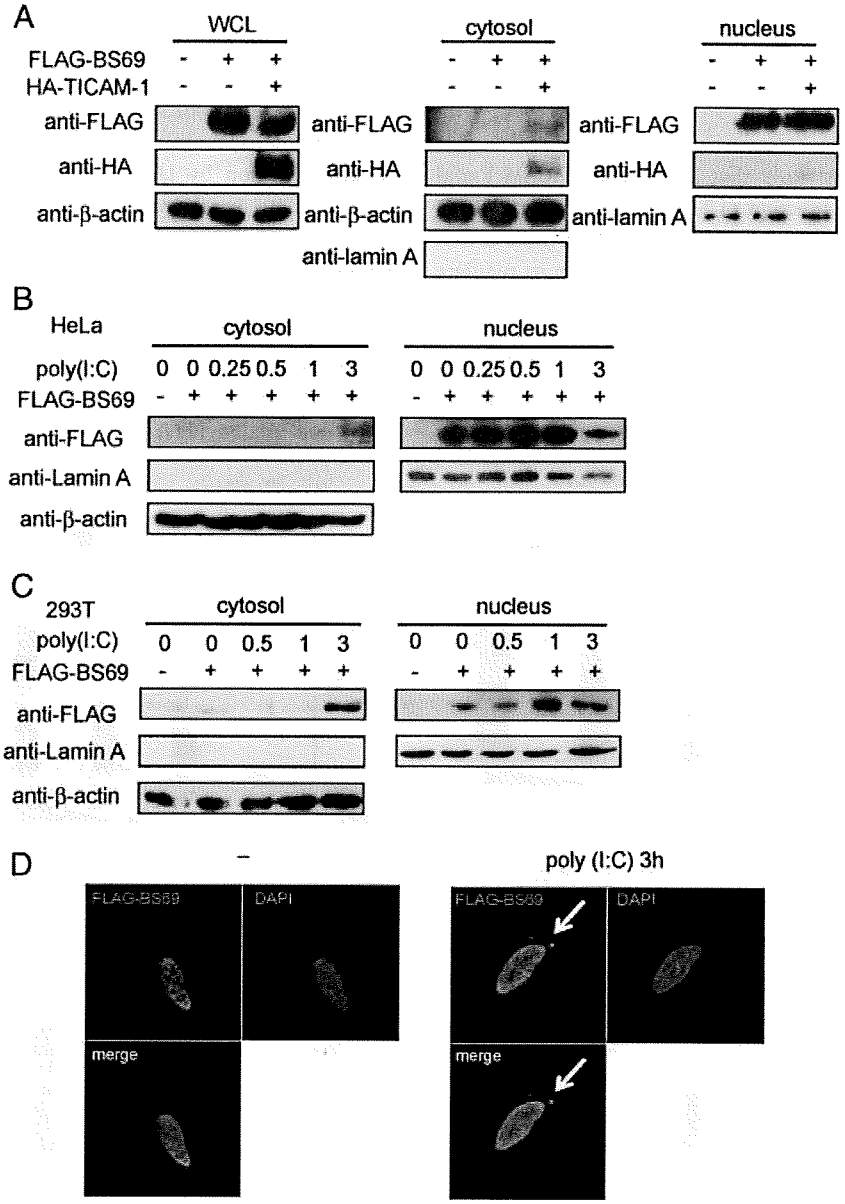

Figure 3. TICAM-1 over-expression induces cytoplasmic translocation of BS69. (A) HEK 293T cells were transfected with 1 ng of pEF-BOS HA-TICAM-1 WT and 100 ng of pEF-BOS FLAG BS69. After 24 h, the cells were lysed and cytoplasmic and nuclear extractions were prepared. Each extraction was resolved by SDS-PAGE and immunoblotted with either anti-HA, anti-FLAG anti-β-actin or anti-Lamin A (as a nuclear marker) Ab. (B) HeLa cells were transfected with 1 μg of pEF-BOS FLAG-BS69. After 24 h, the cells were stimulated with 10 μg/mL of polyI:C for either 0, 0.25, 0.5, 1 or 3 h. The cytoplasmic and nuclear extractions were then prepared, run on SDS-PAGE gels and immunoblotted with either anti-FLAG, anti-β-actin or anti-Lamin A (as a nuclear marker) Ab. (C) HEK293T cells were transfected with 100 ng of pEF-BOS FLAG-BS69 and 100 ng of pEF-BOS human TLR3. After 24 h, the cells were stimulated with 50 μg/mL of polyI:C for the indicated periods. The cytosolic and the nuclear extractions were analyzed as shown in (B). (D) HeLa cells were transfected with 400 ng of pEF-BOS FLAG-BS69. After 24 h, the cells were stimulated with 10 μg/mL of polyI:C for 3 h. Thereafter, the cells were fixed and stained with anti-FLAG Ab and visualized with Alexa Fluor 594-conjugated secondary Ab. The same slide was also treated with DAPI for the staining of nuclei. The white arrows indicate BS69 cytoplasmic speckles.

were quantitatively measured in cells expressing BS69 after polyI:C stimulation (Fig. 4D). The levels of mRNA significantly increased at 6 and 12 h after polyI:C stimulation in the BS69-transfected cells in comparison with cells containing the control vector. We next introduced an siRNA of BS69 into HeLa cells and examined polyI:C-mediated IFN-β induction. The IFN-β mRNA level induced by polyI:C dropped down by the presence of the siRNA (Supporting Information Fig. S1). The data suggest that BS69 acts as a positive regulator of the TICAM-1 pathway in both NF-κB activation and IFN-β induction through its trafficking from the nucleus to the cytoplasm.

Discussion

We demonstrated in this study that BS69 binds TICAM-1 and positively modulates the function of TICAM-1 in terms of NF-κB and IRF-3 activation. BS69 is essentially a nuclear protein that can be displaced from the nucleus to the cytoplasm to regulate TICAM-1 signaling. Either low doses of polyI:C stimulation or TICAM-1 expression induces BS69 translocation, whereas high TICAM-1 expression leads to the disappearance of the nuclear and cytosolic BS69, presumably due to apoptosis (data not shown). BS69 not only augments the TICAM-1 pathway *via* its binding to TCAM-1, but also participates in BS69 nucleus-to-cytoplasm displacement.

BS69 is a 74-kDa protein with three truncated isoforms that are formed through alternative splicing [5]. All four forms are unstable as they can be easily degraded by post-translational modification through the proteasome pathway [5]. Our preliminary data suggest that protein modification, particularly one other than ubiquitination, participates in the degradation of BS69 (data not shown). This is consistent with the finding that high doses of TICAM-1 induce the activation of TRAF E3 ligases [11] and protein modification [12], though the mechanisms have yet to be determined.

The previous reports have demonstrated that BS69 physically binds EBV-derived LMP1 and negatively regulates the canonical NF-κB activation by LMP1 [10, 13]. Although the regulatory mode of LMP1 is reciprocal to that of TICAM-1, the extranuclear displacement of BS69 commonly occurs in polyI:C- and LMP1-activating pathways. Thus, BS69 exerts a functional modulation of NF-κB in at least in two cytoplasmic pathways: positive regulation in the TICAM-1 pathway and negative regulation in the LMP1 pathway.

TICAM-1 recruits TRAF1, TRAF2 and TRAF6 to sites within its N-terminal region [11], and TRAF3 indirectly couples with the

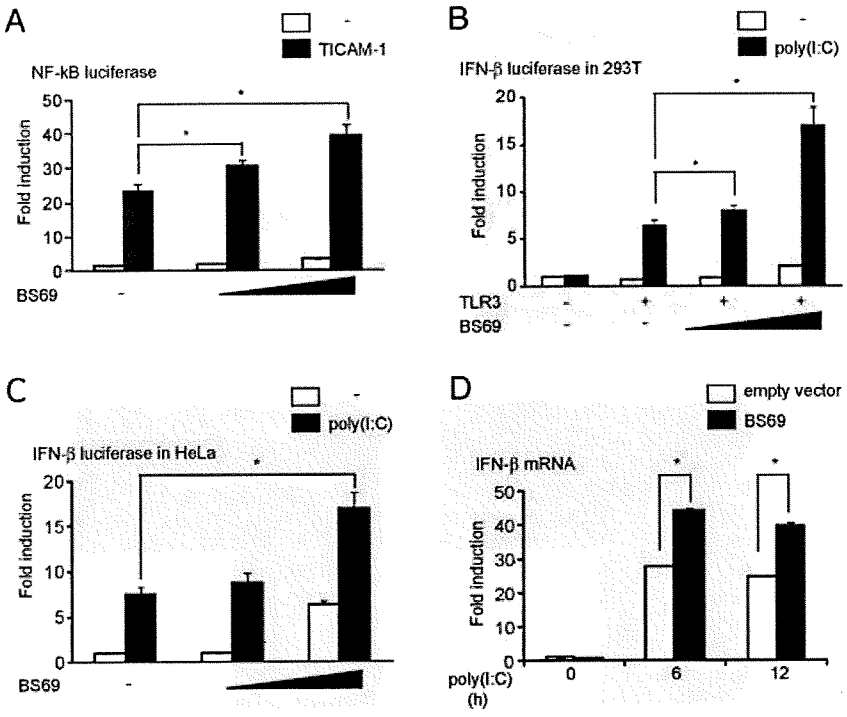

Figure 4. BS69 is a positive regulator of the TICAM-1 pathway. (A) HEK 293T cells in 24-well plates were transfected with pEF-BOS FLAG-BS69 (10, 100 ng) together with pEF-BOS HA-TICAM-1 WT (100 ng), the NF-κB reporter (100 ng) and phRL-TK (5 ng). Twenty-four hours after transfection, the luciferase reporter activity was measured. The average activities from three independent assays are shown as fold induction. (B) HEK 293T cells were transfected with pEF-BOS FLAG-BS69 (10, 100 ng) together with pEF-BOS TLR3 (10 ng), the IFN-β promoter reporter (100 ng) and phRL-TK (5 ng). After 24 h, the cells were stimulated with 10 μg/mL polyI:C for 6 h and the luciferase reporter activity was then measured. The average activities from three independent assays are shown as fold induction. (C) HeLa cells in 24-well plates were transfected with pEF-BOS FLAG-BS69 (10,100 ng) together with the IFN-β promoter reporter (100 ng) and phRL-TK (5 ng). Twenty-four hours after transfection, the cells were stimulated with 10 μg/mL polyI:C for 6 h, and then the luciferase reporter activity was measured. The average activities from three independent assays are shown as fold induction. (D) HeLa cells in 12-well plates were transfected with either pEF-BOS FLAG-BS69 (1 μg) or empty vector (1 μg). After 24 h, the cells were stimulated with 10 μg/mL polyI:C for the indicated time periods. The IFN-β mRNA levels were determined by real-time PCR. *$p<0.05$.

molecular complex of these proteins [14, 15]. NAP1 also bind indirectly to the N-terminus of TICAM-1 [3]. Thus, the visible TICAM-1 multimer observed by confocal analysis is likely a signal platform directing the activation of IRF-3-activating kinases and IκB degradation kinases [4]. From our data, we can infer that when an optimal stimulus, such as an RNA viral infection, is present in the target cells, two molecular events are independently triggered: BS69 translocation to the cytoplasm and TICAM-1 signalosome formation. These two events could be simultaneously reproduced in our system, resulting in the up-regulation of the TICAM-1 inflammatory pathway.

Upon infection of a cell by EBV, the EBV product LMP1 induces NF-κB and JNK activation. This LMP1-derived NF-κB activation is negatively regulated by BS69 [10] coping with internal TLR3 signaling. Radical activation of the TICAM-1 pathway, however, is not supported by BS69-mediated NF-κB up-regulation as BS69 is degraded *via* post-translational modification. This is in accordance with the fact that full length TICAM-1 occasionally induces apoptotic cell death, which reflects a natural feature of the antiviral response.

The previous studies have demonstrated that BS69 acts as a transcriptional repressor in association with a variety of transcription factors such as c-Myb, B-Myb, Ets2 and MGA [7, 16, 17]. BS69 has also been shown to repress transcription by recruiting N-CoR [6]. A recent study suggested that BS69 has another role in gene repression since it co-precipitates with a set of chromatin remodeling factors and interacts with the transcription factor ZHX1 [18]. Furthermore, BS69 has been shown to associate with mitotic chromosomes and to interact with Brg1 (the catalytic subunit of the mammalian SWI/SNF complex), indicating an additional role of BS69 in chromatin remodeling [19]. In either case, it is clear that BS69 functions in the nucleus. As a sensitive Ab against BS69 is not available, it is extremely difficult to detect endogenous BS69 protein in the cytoplasm. However, our studies, together with a report on BRAM1, a truncated form of BS69 which displaces TRADD from LMP1 to inhibit LMP1-mediated NF-κB activation [10], indicate that BS69 plays a role in the cytoplasm to modulate inflammation secondary to viral infection. In keeping with its NF-κB modulating function and chromatin-associated properties, BS69 is a bifunctional protein acting in the nucleus and cytoplasm to maintain the homeostasis of the cellular environment.

In mDC, TICAM-1 has a unique role in driving cellular immunity as $CD8^+$ T, $CD4^+$ Treg, Th1, Th17 and NK cells are all activated in response to TICAM-1-mediated mDC maturation [1, 20]. We found the TICAM-1 pathway in mDC is activated *via* endosomal TLR3 through the phagocytic uptake of viral-infected cell debris [21]. Our data suggest the possibility that BS69 is an agent used to regulate the induction of TICAM-1-mediated cellular immunity in addition to the NF-κB- and IFN-activating pathways. More detailed analysis of endogenous TLR-associated proteins and BS69/BRAM1, including *in vivo* functional analysis, will be needed in order to highlight the precise cytoplasmic function(s) of BS69.

Materials and methods

Cell culture and reagents

HEK293 T cells were maintained in DMEM supplemented with 10% heat-inactivated FBS and antibiotics. HeLa cells were cultured in Eagle's MEM with 10% heat-inactivated FBS and L-glutamine. The following Ab were obtained commercially: anti-FLAG, anti-HA and anti-β-actin (Sigma-Aldrich); anti-Myc (Santa Cruz); anti-Lamin A (Cell Signaling Technology). Alexa Fluor 488- and Alexa Fluor 568-conjugtaed secondary Ab were from Invitorgen Life Technologies. polyI:C was from Amersham Biosciences.

Plasmids

Complementary DNA from human TLR3, TICAM-1WT, TICAM-1 N+TIR P434H and RHIM mt were cloned in our laboratory by RT-PCR and ligated into the cloning site of the expression vector, pEF-BOS and pcDNA4 Myc-HisA [4]. BS69 cDNA was cloned as described previously [11]. Mutations were introduced by site-directed mutagenesis using PCR. [3]. All constructs were confirmed by sequencing.

Confocal microscopy

HeLa cells (2.5×10^4 cells/well) were plated on a micro cover glass (Matsunami Glass) in 12-well plate. The following day, cells were transfected with the indicated plasmids using FuGENE HD (Roche). The total amounts of DNA were kept constant by adding empty vector. After 24 h, cells were fixed in acetone and blocked in PBS containing 1% BSA and then labeled with the indicated primary Ab for 1 h at room temperature. Alexa Fluor 488- or Alexa Fluor 594-conjugtaed secondary Ab were used for the visualizing proteins detected by the primary Ab. For nucleus staining, cells were treated with DAPI in PBS. After all staining procedures were finished, micro cover glasses were mounted onto a slide glass using PBS containing 2.3% DABCO and 50% glycerol. Cells were visualized at ×63 magnification under an LSM510 META microscope (Zeiss).

Reporter gene assay

Cells were seeded onto 24-well plates and transfected with various amounts of expression vectors, the reporter gene and the phRL-TK control plasmid using FuGene HD (Roche) according to the manufacturer's instructions. After 24 h, the cells were harvested in 50 μL lysis buffer. The luciferase activity was measured using Dual-Luciferase Reporter assay systems (Promega) and was shown as the means ± SD of three experiments.

Western blotting and immunoprecipitation assay

For whole cell lysis, cells were solubilized in the SDS sampling buffer (50 mM Tris-HCl, pH 6.8, 2% SDS, and 10% glycerol, 32% Urea) and then sonicated for 5 min. For cytosol extraction, cells were solubilized in the lysis buffer A (10 mM HEPES-KOH, pH 7.9, 150 mM NaCl, 15 mM $MgCl_2$, 10 mM KCl, 40 mg/mL digitonin, protease inhibitor cocktail, 0.1 mM PMSF, 50 mM NaF and 1 mM Na_3VO_4) on ice for 30 min and then centrifuged at 10 000 × *g* for 1 min at 4°C. The supernatant was collected as a cytosol extraction. After centrifugation, the nuclei-containing pellet was resuspended in the buffer C (50 mM HEPES-KOH (pH 7.9), 420 mM KCl, 1.5 mM $MgCl_2$, 1 mM EDTA, 2% glycerol, protease inhibitor cocktail, 0.1 mM PMSF, 50 mM NaF and 1 mM Na_3VO_4) at 4°C for 30 min. The suspension was pelleted by centrifugation and the supernatants were collected as a nuclear extraction. The supernatants were separated by SDS-PAGE, and the gel was transferred onto polyvinylidene difluoride membranes. The membranes were then blocked with TBS, pH 8.0, containing 5% skim milk, immunoblotted with specific Ab and visualized with the appropriate horseradish peroxidase-conjugated secondary Ab using the ELC plus Western Blotting Detection System (Amersham Pharmaica). For immunoprecipitation, cells were lysed in the TritonX-100 lysis buffer (50 mM Tris-HCl, pH 7.4, 150 mM NaCl, 1.5 mM $MgCl_2$, 1% TritonX-100, 10% glycerol, protease inhibitor cocktail, 0.1 mM PMSF, 50 mM NaF and 1 mM Na_3VO_4) and then centrifuged at 12 000 × *g* for 10 min at 4°C. The supernatants were incubated with anti-FLAG or anti-Myc Ab and protein G-Sepharose (Amersham Pharmacia) for overnight at 4°C. The immunoprecipitates were collected by centrifugation, washed four times in the lysis buffer and then analyzed by SDS-PAGE.

RNA purification and real-time PCR

Total RNA was prepared using TRIzol Reagent (Invitrogen) following the manufacturer's instructions. RT-PCR was carried out using the High Capacity cDNA Reverse Transcripition kit (Applied Biosystems) according to the manufacturer's instructions. The following oligonucleotides were used for human β-actin: 5′-CCT GGC ACC CAG CAC AAT-3′ and 5′-GCC GAT CCA CAC ACG GAG TAC T-3′; and for human IFN-β: 5′-TGG GAG GAT TCT GCA TTA CC-3′ and 5′-CAG CAT CTG CTG GTT GAA GA-3′; and for human BS69: 5′-GTC CAC GGT ATG CAC CCT AAA GAG and 5′-AAC ACC TCT CCA GGC AAA TGG. IFN-β mRNA were normalized to β-actin and fold inductions of transcripts were calculated using the δδCT method relative to unstimulated HeLa cells.

Yeast two-hybrid screening

The yeast two-hybrid assay was performed as described previously [12]. The yeast AH109 strain (Clontech, Palo Alto, CA, USA) was transformed using bait (pGBKT7) and prey (pGADT7) plasmids. The transformants were streaked onto plates and incubated for 3–5 days. and in the figures represent the bait and prey plasmid, respectively. The various BD-TICAM-1 and AD-BS69 were constructed by inserting each cDNA fragment into the pGBKT7 (bait) or pGADT7 (prey) plasmids (Clontech). SD-WLH is a yeast synthetic dextrose medium that lacks Trp, Leu and His aa. SD-WLHA lacks adenine in addition to Trp, Leu and His.

Gene silencing

Knockdown of BS69 was carried out using siRNA, BS69 siRNA-1: 5′-GGA UAU UGG CCA GGA GTT-3′, BS69 siRNA-2: 5′-CGG UAU GCA CCC UAA AGA GTT-3′ and control siRNA: 5′-GGG AAG AUC GGG UUA GAC UUC-3′. In total, 20 pmol of each siRNA was transfected into HeLa cells in 24-well plate with Lipofectamin 2000 according to the manufacture's protocol. Knockdown of BS69 was confirmed 48 h after siRNA transfection. Experiments were repeated twice for confirmation of the results. One of the two siRNA, BS69 siRNA-1 was effective in BS69 gene silencing. Typically, 6 h after polyI:C (10 μg/mL) stimulation, the level of the BS69 mRNA was determined by real-time PCR as described in RNA purification and real-time PCR section.

Acknowledgements: The authors thank the members of our laboratory for invaluable discussions. This work was supported in part by the Program of Founding Research Centers for Emerging and Reemerging Infectious Diseases, MEXT, Sapporo Biocluster "Bio-S", the Knowledge Cluster Initiative of the MEXT, Grants-in-Aid from the Ministry of Education, Science, and Culture (Specified Project for Advanced Research) and the Ministry of Health, Labor, and Welfare of Japan, Mitsubishi Foundation, Mochida Foundation, NorthTec Foundation and Yakult Foundation. M. S. was supported by Reseach Fellow of the Japan Sciety for the Promotion of Science. Dr. Greg Newton (NEWTONediting) reviewed the manuscript.

Conflict of interest: The authors declare no financial or commercial conflict of interest.

References

1 **Matsumoto, M. and Seya, T.,** TLR3: interferon induction by double-stranded RNA including poly(I:C). *Adv. Drug Deliv. Rev.* 2008. **60**: 805–812.

2 **Matsumoto, M., Funami, K., Tanabe, M., Oshiumi, H., Shingai, M., Seto, Y., Yamamoto, A. and Seya, T.,** Subcellular localization of Toll-like receptor 3 in human dendritic cells. *J. Immunol.* 2003. **171**: 3154–3162.

3 **Funami, K., Sasai, M., Ohba, Y., Oshiumi, H., Seya, T. and Matsumoto, M.,** Spatiotemporal mobilization of Toll/1L-1 receptor domain-containing

adaptor molecule-1 in response to dsRNA. *J. Immunol.* 2007. **179**: 6867–6872.

4 **Funami, K., Sasai, M., Oshiumi, H., Seya, T. and Matsumoto, M.,** Homo-oligomerization is essential for Toll/IL-1 receptor domain containing adaptor molecule-1-mediated NF-kappaB and interferon regulatory factor-3 activation. *J. Biol. Chem.* 2008. **283**: 18283–18291.

5 **Velasco, G., Grkovic, S. and Ansieau, S.,** New insights into BS69 functions. *J. Biol. Chem.* 2006. **281**: 16546–16550.

6 **Masselink, H. and Bernards, R.,** The adenovirus E1A binding protein BS69 is a corepressor of transcription through recruitment of N-CoR. *Oncogene* 2000. **19**: 1538–1546.

7 **Ladendorff, N. E., Wu, S. and Lipsick, J. S.,** BS69, an adenovirus E1A-associated protein, inhibits the transcriptional activity of c-Myb. *Oncogene* 2001. **20**: 125–132.

8 **Ansieau, S. and Leutz, A.,** The conserved Mynd domain of BS69 binds cellular and oncoviral proteins through a common PXLXP motif. *J. Biol. Chem.* 2002. **277**: 4906–4910.

9 **Izumi, K. M., Cahir McFarland, E. D., Ting, A. T., Riley, E. A., Seed, B. and Kieff, E. D.,** The Epstein-Barr virus oncoprotein latent membrane protein 1 engages the tumor necrosis factor receptor-associated proteins TRADD and receptor-interacting protein (RIP) but does not induce apoptosis or require RIP for NF-κB activation. *Mol. Cell. Biol.* 1999. **19**: 5759–5767.

10 **Ikeda, O., Sekine, Y., Mizushima, A., Oritani, K., Yasui, T., Fujimuro, M., Muromoto, R. *et al.*,** BS69 negatively regulates the canonical NF-kappaB activation induced by Epstein-Barr virus-derived LMP1. *FEBS Lett.* 2009. **583**: 1567–1574.

11 **Sasai, M., Oshiumi, H., Funami, K., Matsumoto, M. and Seya, T.,** Direct binding of TRAF2 and TRAF6 to TICAM-1/TRIF adaptor of the Toll-like receptor 3/4 pathway. *Mol. Immunol.* 2009, in press.

12 **Oshiumi, H., Matsumoto, M., Funami, K., Akazawa, T. and Seya, T.,** TICAM-1, an adapter molecule that participates in Toll-like receptor 3-mediated interferon-beta induction. *Nat. Immunol.* 2003. **4**: 161–167.

13 **Wan, J., Zhang, W., Wu, L., Bai, T., Zhang, M., Lo, K. W., Chui, Y. L. *et al.*,** BS69, a specific adaptor in the latent membrane protein1-mediated c-Jun N-terminal kinase pathway. *Mol. Cell. Biol.* 2006. **26**: 448–456.

14 **Häcker, H., Redecke, V., Blagoev, B., Kratchmarova, I., Hsu, L. C., Wang, G. G., Kamps, M. P. *et al.*,** Specificity in Toll-like receptor signalling through distinct effector functions of TRAF3 and TRAF6. *Nature* 2006. **439**: 204–207.

15 **Oganesyan, G., Saha, S. K., Guo, B., He, J. Q., Shahangian, A., Zarnegar, B., Perry, A. and Cheng, G.,** Critical role of TRAF3 in the Toll-like receptor-dependent and -independent antiviral response. *Nature* 2006. **439**: 208–211.

16 **Wei, G., Schaffner, A. E., Baker, K. M., Mansky, K. C. and Ostrowski, M. C.,** Ets-2 interacts with co-repressor BS69 to repress target gene expression. *Anticancer Res.* 2003. **23**: 2173–2178.

17 **Masselink, H., Vastenhouw, N. and Bernards, R.,** B-myb rescues ras-induced premature senescence, which requires its transactivation domain. *Cancer Lett.* 2001. **171**: 87–101.

18 **Ogata-Kawata, H., Yamada, K., Uesaka-Yoshino, M., Kagawa, N. and Miyamoto, K.,** BS69, a corepressor interacting with ZHX1, is a bifunctional transcription factor. *Front. Biosci.* 2007. **12**: 1911–1926.

19 **Ekblad, C. M., Chavali, G. B., Basu, B. P., Freund, S. M., Veprintsev, D., Hughes-Davies, L., Kouzarides, T. *et al.*,** Binding of EMSY to HP1beta: implications for recruitment of HP1beta and BS69. *EMBO Rep.* 2005. **6**: 675–680.

20 **Seya, T. and Matsumoto, M.,** The extrinsic RNA-sensing pathway for adjuvant immunotherapy for cancer. *Cancer Immunol. Immunother.* 2009. **58**: 1175–1184.

21 **Ebihara, T., Shingai, M., Matsumoto, M., Wakita, T. and Seya, T.,** Hepatitis C virus (HCV)-infected hepatocytes extrinsically modulate dendritic cell maturation to activate T cells and NK cells. *Hepatology* 2008. **48**: 48–58.

Abbreviations: **BS69:** adenovirus 5 E1A-binding protein · **IRF:** IFN-regulatory factor · **LMP1:** latent membrane protein 1 · **mDC:** myeloid dendritic cells · **mt:** mutant · **TICAM-1:** Toll-interleukin 1 receptor domain (TIR)-containing adaptor molecule-1

Full correspondence: Dr. Tsukasa Seya, Department of Microbiology and Immunology, Hokkaido University Graduate School of Medicine, Kita 15, Nishi 7, Kita-ku Sapporo 060-8638, Japan
Fax: +81-11-706-7866
e-mail: seya-tu@pop.med.hokudai.ac.jp

Current address: Miwa Sasai, Department of Immunobiology, Yale University School of Medicine, New Haven, CT 06510, USA

Supporting Information for this article is available at www.wiley-vch.de/contents/jc_2040/2009/39878_s.pdf

Received: 6/8/2009
Revised: 3/9/2009
Accepted: 3/9/2009

DOI: 10.1002/cbic.200900242

Lipopeptides from *Staphylococcus aureus* as Tlr2 Ligands: Prediction with mRNA Expression, Chemical Synthesis, and Immunostimulatory Activities

Yukari Fujimoto,[a] Masahito Hashimoto,[b] Maiko Furuyashiki,[b] Mami Katsumoto,[a] Tsukasa Seya,[d] Yasuo Suda,[b, c] and Koichi Fukase*[a]

Innate immune receptors recognize particular structurally conserved molecules common to microbes[1] and activate the host's immune response. Toll-like receptor 2 (TLR2) is a member of the TLR family, which encompasses the major innate immune receptors in vertebrates. TLR2 ligands have been reported from diverse microorganisms, although the activity of some ligands as TLR2 agonists is in dispute.[2] Bacterial lipoproteins/lipopeptides are one class of compounds that are generally accepted to be TLR2 ligands. Lipoproteins from the outer membrane of the Gram-negative bacteria, *Escherichia coli*, were shown to be potent activators of B lymphocytes and macrophages.[3,4] These lipoproteins have an *S*-(dihydroxypropyl)cysteine at the N terminus where two hydroxyl groups and an amine group are linked to fatty acids, such as palmitic acid.[5] Jung and co-workers synthesized *N*-palmitoyl-*S*-[2,3-bis(palmitoyloxy)propyl]cysteine (Pam_3Cys) and demonstrated that its bioactivities, including TLR2 activation, are comparable to the native lipoprotein.[6] MALP-2, *S*-[2,3-bis(palmitoyloxy)propyl]cysteinyl-GNNDESNISFKEK, a lipopeptide from *Mycoplasma fermentans* was the only natural TLR2 ligand to be isolated and structurally determine[7,8] until the recent studies of lipoproteins from *Staphylococcus aureus*—a Gram-positive bacteria—by our group and Lee et al.[9,10] Some lipoproteins from other mycoplasma and Gram-negative bacteria have also been studied and the lipopeptide moieties have been chemically synthesized, including *S*-[2,3-bis(palmitoyloxy)propyl]cysteinyl-GDPKHPKSF (FSL-1) from the lipoprotein Lp44 from *Mycoplasma salivarium*[11] and *S*-[2,3-bis(palmitoyloxy)propyl]-*N*-palmitoylcysteinyl-SSNKIDELSSD in the murein lipoprotein from the outer membrane of *E. coli*.[5]

Lipoproteins from Gram-positive bacteria have not been extensively examined in comparison to those from Gram-negative bacteria, with the exception of a study from Sutcliffe and Russell.[12] Götz and co-workers showed that a *S. aureus* lipoprotein diacylglyceryl transferase (*lgt*) deletion mutant, which was deficient in lipidation of prelipoproteins, was attenuated in growth and immune activation.[13] We have demonstrated that degradation of the lipid linkage in lipopeptides/proteins from lipoteichoic acid (LTA) fractions results in decreased TLR2 stimulation, although LTA itself does not have the same kind of lipid linkage.[14–16] A similar tendency has also been reported for TLR2 stimulatory activity of peptidoglycan (PGN) after degradation of the lipid linkage.[2] The intractability of lipoprotein/lipopeptide isolation, which has led to confusion in other investigations of TLR2 ligands, presumably derives from amphiphilicity and the tendency for lipoproteins/lipopeptides to associate with various cell surface components. In order to overcome these difficulties, we have recently succeeded in the identification of TLR2 ligands in Gram-positive bacteria[9] by isolating lipoproteins that showed potent TLR2 stimulatory activity from the lipoteichoic acid (LTA) fraction of TLR2-stimulated *S. aureus*.

In the study described here, we predicted a set of all possible sequence variations of lipoproteins in *S. aureus* that contained the consensus sequence of the protein at the N terminus and studied the expression levels of the mRNA for these predicted lipoproteins. Based on the results of this expression assay, we chemically synthesized sixteen lipopeptides, which contained the *S*-[2,3-bis(palmitoyloxy)propyl]cysteine moiety (Pam_2Cys). The diacylated structure was suggested by the lack of lipoprotein *N*-acyltransferase (Int) in *S. aureus*.[17,18] The Int protein is responsible for fatty acid acylation of the N terminus of the diacylglyceryl-modified cysteine to give the triacylated structure. This is in agreement with our results that isolated lipoproteins from *S. aureus* are diacylated,[9] although a triacylated SitC lipoprotein TLR2 ligand from *S. aureus* was also recently reported.[10] In this study, based on the predicted sequences of the lipoproteins, we chemically synthesized diacylated lipopeptides and evaluated their immunostimulatory activity in TLR2-expressing cells and human peritoneal blood mononuclear cells (PBMC).

Based on the results of the RNA-expression experiments, the following lipopeptides were synthesized as the TLR2 candidates of *S. aureus* (Table 1), which include the previously isolated lipoproteins SAOUHSC_00634, _00844, _01002, _01180, _02650, and _02699 from *S. aureus* NCTC8325 from our earlier report.[9] The synthesized compounds contained the Pam_2Cys structure.

First we predicted the lipoproteins from *S. aureus* NCTC8325 using a database of bacterial lipoproteins (DOLOP),[19] which is an application that can be used to predict lipoproteins from completely sequenced bacterial genomes based on the con-

[a] *Prof. Dr. Y. Fujimoto, M. Katsumoto, Prof. Dr. K. Fukase*
Department of Chemistry, Graduate School of Science
Osaka University, Toyonaka, Osaka 560-0043 (Japan)
Fax: (+81) 6-6850-5391
E-mail: koichi@chem.sci.osaka-u.ac.jp

[b] *Prof. Dr. M. Hashimoto, M. Furuyashiki, Prof. Dr. Y. Suda*
Department of Nanostructure and Advanced Materials
Kagoshima University, Kagoshima 890-0065 (Japan)

[c] *Prof. Dr. Y. Suda*
Department of Microbiology and Immunology
Graduate School of Medicine, Hokkaido University
Sapporo 060-8638 (Japan)

[d] *Prof. Dr. T. Seya*
Venture Business Laboratory, Kagoshima University
Kagoshima 890-0065 (Japan)

Supporting information for this article is available on the WWW under http://dx.doi.org/10.1002/cbic.200900242.

Table 1. Synthesized lipopeptide structures and the functions and expression levels of the original proteins.

Lipopeptide	Structure	SAOUHSC number of original proteins	Putative function of proteins[13]	Expression level of RNA
LPSA-01	Pam_2CANTRHSESDK	_186	ABC-type Fe^{3+} transporter	±
LPSA-02	Pam_2CGTGGKQSSDK	_634	ABC transporter, SitC	+++
LPSA-03	Pam_2CGNGNKSGSDD	_844	NLPA lipoprotein	+
LPSA-04	Pam_2CSNIEIFNAKG	_1002	probable quinol oxidase subunit 2 (qoxA)	++++
LPSA-05	Pam_2CTTDKKEIKAY	_1039	uncharacterized protein	±
LPSA-06	Pam_2CSFGGNHKLSS	_1180	uncharacterized protein	±
LPSA-07	Pam_2CGSQNLAPLEE	_1627	galactoside ABC transporter, permease protein	+
LPSA-08	Pam_2CGQDSDQQKDG	_2650	uncharacterized lipoprotein	++
LPSA-09	Pam_2CGNDDGKDKDG	_2690	ABC-type Zn^{2+} transporter	±
LPSA-10	Pam_2CGNNSSKDKEA	_2699	ABC-type amino acid transporter	++
LPSA-11	Pam_2CSLPGLGSKST	_2742	ABC-type glycine betaine transporter	+
LPSA-12	Pam_2CSTSEVIGEKI	_2355	uncharacterized protein (UPF0340 protein)	++++
LPSA-13	Pam_2CPFNCVGCYNK	_2941	anaerobic ribonucleotide reductase	++++
LPSA-07-2	Pam_2CGSQNLAPLEEK	_1627	galactoside ABC transporter, permease protein	+
LPSA-14	Pam_2CLILIIASETL	_2008	teichoic acid transport protein, TagG	±
LPSA-14-2	Pam_2CLILIIASETLFSFSHLTDVK	_2008		±
Pam_2CSK_4	Pam_2CSKKKK	–	artificial ligand	N/A

sensus sequence at the N terminus of the proteins. We first searched for the consensus sequence ([LVI][ASTVI][ASG][C]) in the full bacterial genome and obtained proteins that were subsequently checked through DOLOP with this sequence at the protein's N terminus. We then analyzed RNA expression of 54 estimated lipoproteins by real-time PCR and the results are shown in the Supporting Information.

Immunostimulating lipopeptides have been prepared previously by Jung and co-workers.[20,21] We here improved the preparation of the diacylglycerylmodified cysteine residue and the construction of the lipopeptide, and we synthesized lipopeptides with natural amino acid sequences from *S. aureus* NCTC8325. The synthesis of lipopeptides was achieved with a combination of solution- and solid-phase methods (Scheme 1). For the preparation of the Pam_2Cys backbone, the protected cysteine **1** and the iodide **2**[22] were coupled under basic condition by using Cs_2CO_3 to give **3**, and the subsequent acylation and cleavage of the *t*Bu group gave Fmoc-Pam_2Cys-OH (**5**). Cysteine **1** was prepared from the

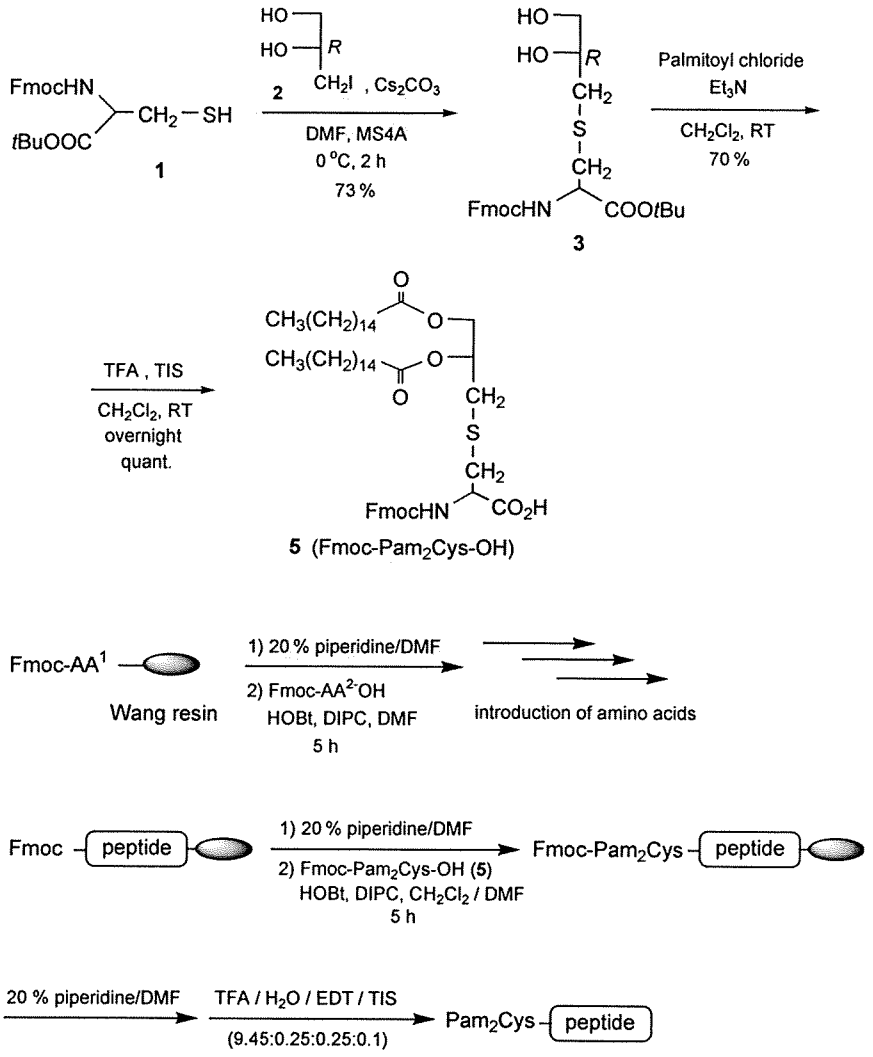

Scheme 1. Chemical synthesis of lipopeptides LPSA-01–LPSA-14-2 and Pam_2CSK_4.

corresponding protected cystine by reduction with Zn in AcOH.[23] The peptide component, which included 16 different peptide sequences from 14 lipoproteins of *S. aureus* NCTC8325, was prepared by using solid-phase synthesis on Wang resin in a similar fashion to Jung's lipopeptide synthesis.[20,21] Fmoc-Pam_2Cys-OH (**5**) was then introduced to the N terminus of the peptides linked to the resin. Subsequent cleavage of the Fmoc group, detachment from the resin, and deprotection of all protecting groups gave the lipopeptides LPSA-01–14-2, and also Pam_2CSK_4.

Receptor activation (TLR2, TLR4/MD2) and cytokine (TNF-α) induction activities of the synthesized lipopeptides were studied. All lipopeptides activated TLR2 expressing cells (Ba/mTLR2; Figure 1 A) but did not activate either the murine TLR4 and MD-2 expressing cells Ba/mTLR4/mMD-2 or the negative control Ba/κB cells (data not shown). Activity levels varied according to peptide sequence, with the most active lipopeptides being LPSA-01, -02, -08, and -12. LPSA-04, -13, and -14 showed relatively much weaker activities. The lipopeptides also dose dependently stimulated human PBMC to induce TNF-α (Figure 1 B) and the trends of the stimulatory activities were similar except that some lipopeptides, such as LPSA-01, -02, and -07-2, showed relatively weaker activities.

The weaker immunostimulatory activity of LPSA-13 was presumably caused by conformational distortion of the proline residue proximal to the Pam_2Cys. In the case of LPSA-04, -13, -14, and the 20-residue fragment of LPSA-14, LPSA-14-2, the hydrophobic properties of the peptides would be expected to decrease activity.

The chemically synthesized lipopeptide fragments of *S. aureus* all activated TLR2-expressing cells (Ba/mTLR2; Figure 1 A), but activity levels varied in a similar way to their respective TNF-α induction. The structure–activity relationships are currently under investigation with both immunological and structural biology methods.

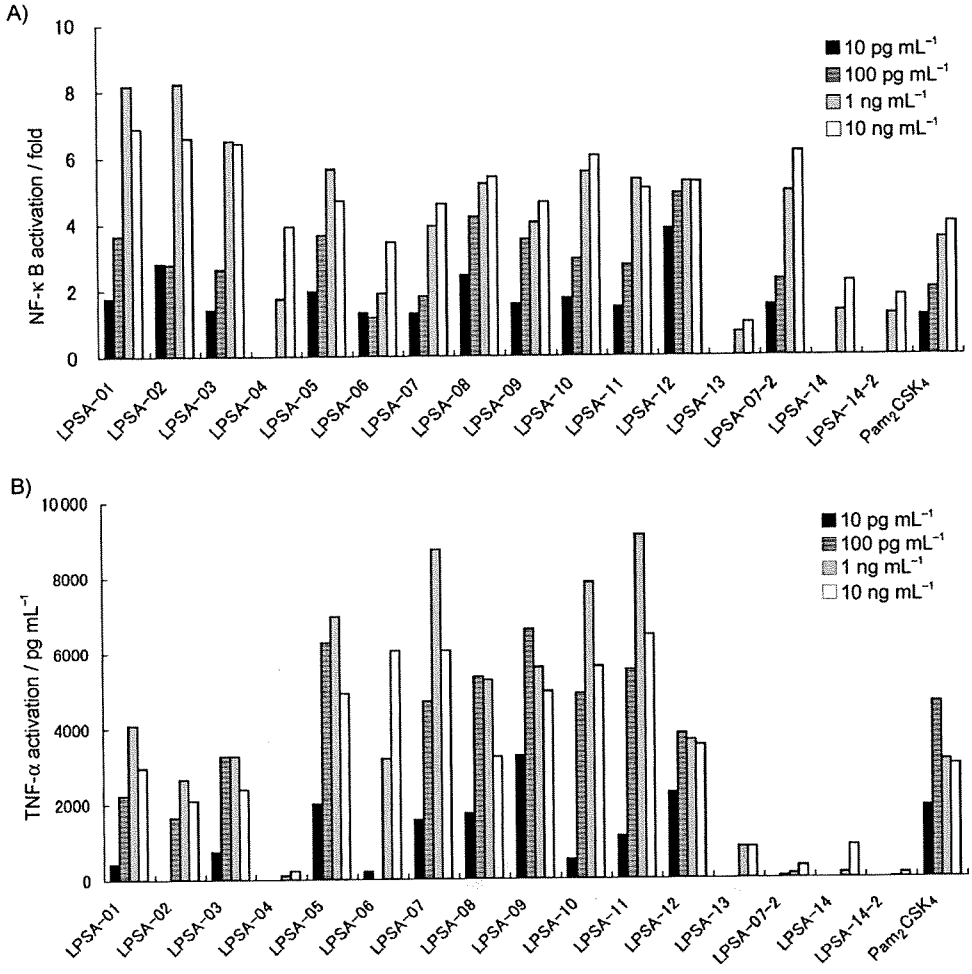

Figure 1. A) TLR2 stimulatory activities of synthesized lipopeptides LPSA-01–LPSA-14-2 and Pam_2CSK_4. NF-κB-dependent luciferase activities in murine TLR2-expressing Ba/F3 cells (Ba/mTLR2) was determined. B) TNF-α stimulatory activities of the synthesized lipopeptides. The lipopeptides were incubated with human PBMCs and cytokine production was determined by ELISA.

Two natural lipoproteins, diacylated SAOUHSC_02699[9] and triacylated SAOUHSC_00634 (SitC),[10] have been previously isolated independently. Here, we report the synthesis of the diacylated lipopeptide LPSA-02 (a fragment of SAOUHSC_00634 (SitC)) and LPSA-10 (a fragment of SAOUHSC_02699). The TNF-α induction and TLR2 activation of LPSA-10 resembled the activities of the lipoprotein SAOUHSC_02699.

In conclusion, we examined the expression levels of the mRNA for a set of predicted lipoproteins from *S. aureus*. Based on the results of the RNA-expression experiments and our recent studies of isolated lipoproteins, we chemically synthesized sixteen lipopeptide fragments and observed TLR2 recognition and immunostimulatory activities. The results show that all fragments activated TLR2-expressing cells and also stimulated human PBMC to induce TNF-α, although the amino acid sequences of the peptide component significantly affected activity levels. The molecular basis of the immunostimulatory activities is currently under investigation. Our results indicate that a number of lipoproteins on the cell surface of *S. aureus* stimulate TLR2, and N-terminal amino acid sequences of the lipoproteins affect immunostimulatory activity, which presumably relates to the virulence of Gram-positive bacteria.

Experimental Section

Prediction of lipoproteins in *S. aureus*: The genome of *S. aureus* NCTC8325 (CP000253.1) was used for searching genes encoding putative lipoproteins. Proteins containing the lipobox consensus sequence ([LV][ASTVI][GAS][C]) were extracted from the complete genome. The proteins obtained were further confirmed in the online Database of Bacterial Lipoproteins (DOLOP).[19,24]

RNA expression of predicted lipoproteins: *S. aureus* SA113 was grown in brain heart infusion broth (Eiken, Tokyo, Japan) at 37 °C for 3 h at mid-log phase, 5 h at late log phase, 7 h, and 9 h at stationary phase, and harvested by centrifugation. Total RNA was extracted from bacteria by using TRIzol max bacterial RNA isolation kit (Invitrogen, Carlsbad, CA, USA) according to manufacturer's instruction and further treated with DNase (Takara Bio, Shiga, Japan). The mRNAs were reverse transcribed by using RNA PCR Kit (AMV) Ver. 3.0 (Takara Bio) and the cDNAs were analyzed with Q-PCR by using a 7300 real-time PCR system from Applied Biosystems (Foster City, CA, USA) with SYBR® Premix Ex-Taq (Takara Bio) according to manufacturer's instructions. Primer pairs were constructed with the help of the Primer 3 program (http://frodo.wi.mit.edu/). The expression values of lipoprotein genes were normalized to the values determined for the gyrase gene (SAOUHSC_00006). The data represent the mean obtained from three independent experiments.

Chemical synthesis of lipopeptides

*(R)-N-(9H-Fluorenylmethoxycaronyl)-S-[2,3-dihydroxy-(2R)-propyl]cysteine tert-butyl ester, **3***: Cesium carbonate (48.0 mg, 0.148 mmol) was added to a mixture of **2** (30.1 mg, 0.148 mmol), **1** (59.0 mg, 0.148 mmol), and MS4A in dry DMF (1.2 mL) at 0 °C. The reaction mixture was stirred under Ar for 2 h. Citric acid solution (10%, 20 mL) was added and the mixture was extracted with diethyl ether. The combined organic layers were washed with brine, dried over Na_2SO_4, and concentrated in vacuo. The residue was purified by silica gel column chromatography (toluene/EtOAc, 10:1) to give **3** (51.2 mg, 73%) as a white solid.

*(R)-N-(9H-Fluorenylmethoxycaronyl)-S-[2,3-di(palmitoyloxy)-(2R)-propyl]cysteine, **5***: Palmitoyl chloride (34.8 mg, 0.127 mmol) and triethylamine (12.9 mg, 0.127 mmol) were added to a solution of **3** (30.0 mg, 0.0633 mmol) in dry CH_2Cl_2. The mixture was stirred for 4 h under Ar. Citric acid solution (10%) was added and the mixture was extracted with CH_2Cl_2. The combined organic layers were washed with brine, dried over Na_2SO_4, and concentrated in vacuo. The residue was purified by silica gel column chromatography (toluene/EtOAc, 50:1) to give the dipalmitoyl compound (42.1 mg, 70%) as a white solid.

The dipalmytoyl compound (200 mg, 0.21 mmol) was stirred with TFA (400 μL), CH_2Cl_2 (400 μL), and triisopropylsilane (15.5 μL), overnight. The solvent was removed in vacuo and the residue was purified by silica gel column chromatography ($CHCl_3$/methanol, 20:1) to give **5** (165.7 mg, 88%) as a white solid. ESI-MS (negative) *m/z* 892.64 $[M-H]^-$; ^{1}H NMR (500 MHz, $CDCl_3$): δ = 7.76–7.31 (m, 8H; Fmoc-Ar*H*), 5.74 (d, *J* = 5.5 Hz, 1H; FmocN*H*), 5.17 (m, 1H; *S*-glyceryl-C*H*), 4.65 (m, 1H; –NH–*CH*–CO–), 4.41 (m, 1H; *S*-glyceryl-OC*H*H), 4.35 (m, 2H; FmocCH_2), 4.24 (t, *J* = 7.1 Hz, 1H; FmocC*H*), 4.15 (dd, *J* = 6.3, 11.9 Hz, 1H; *S*-glyceryl-OCH*H*), 3.16 (dd, *J* = 3.4, 12.4 Hz, 1H; Cys-C*H*H), 3.07 (dd, *J* = 3.6, 12.9 Hz, 1H; Cys-CH*H*), 2.77 (m, 2H; *S*-glyceryl-CH_2), 2.35–2.26 (m, 4H; Pam-CH_2), 1.63–1.56 (m, 4H; Pam-CH_2), 1.25 (s, 48H; Pam-CH_2), 0.88 (t, *J* = 7.0 Hz, 6H; Pam-CH_3).

Typical procedures of solid-phase synthesis of lipopeptide (LPSA-01)

Introduction of Fmoc-L-Lys(Boc)-OH to solid support and cleavage of Fmoc group: Wang resin (100–200 mesh, Novabiochem; 75.3 mg, 0.07 mmol) was used as a support. Bond Elut reservoir (Varian, Inc.; polypropylene syringe) was used as a reaction vessel. The resin was washed with dry dichloromethane. A solution of Fmoc-L-Lys-(Boc)-OH (164.0 mg, 0.35 mmol), MSNT (103.7 mg 0.35 mmol), 1-methylimidazole (25 mL, 0.315 mmol) in dry dichloromethane (500 mL) was stirred for 1 h, and the solution was added to the reaction vessel. The reaction mixture was shaken, overnight. The resin was filtered, and washed with dry dichloromethane (1 mL, 1 min × 5) and DMF (1 mL, 1 min × 5).

Piperidine (20%) in DMF (1 mL) was added to the peptide-linked resin and shaken for 10 min. The resin was filtered and washed with DMF (1 mL, 1 min). Piperidine (20%) in DMF (1 mL) was added and the mixture was shaken for 30 min. The resin was filtered and washed with DMF (1 mL, 1 min × 5) and dichloromethane (1 mL, 1 min × 5). The reaction was checked by using the bromophenol blue (BPB) test.

Peptide-chain formation: DIPC (32.9 mL, 0.21 mmol) was added to a solution of Fmoc-Asp(O*t*Bu)-OH (86.4 mg, 0.21 mmol), HOBt (28.4 mg, 0.21 mmol) in DMF (500 mL) at 0 °C. The solution was stirred for 1 h under Ar. The mixture was added to the resin in a reaction vessel and shaken for 5 h. The resin was filtered and washed with DMF (1 mL, 1 min × 5) and dichloromethane (1 mL, 1 min × 5). The reaction was checked by using the BPB test. Subsequently, the cleavage of the Fmoc group was carried out. The reaction cycle was repeated by using Fmoc-Ser(*t*Bu)-OH (80.5 mg, 0.21 mmol), Fmoc-Glu(O*t*Bu)-OH (93.1 mg, 0.21 mmol), Fmoc-Ser(*t*Bu)-OH (80.5 mg, 0.21 mmol), Fmoc-His(Trt)-OH (130.1 mg, 0.21 mmol), Fmoc-Arg(pbf)-OH·0.8·IPE (154.7 mg, 0.21 mmol), Fmoc-Thr(*t*Bu)-OH (83.5 mg, 0.21 mmol), Fmoc-Asn(Trt)-OH (125.3 mg, 0.21 mmol), Fmoc-Ala-OH (65.4 mg, 0.21 mmol), with HOBt (each 28.4 mg, 0.21 mmol), DIPC (each 32.9 mL, 0.21 mmol) to give Fmoc-Ala-Asn(Trt)-Thr(*t*Bu)-Arg(pbf)-His(Trt)-Ser(*t*Bu)-Glu(O*t*Bu)-Ser(*t*Bu)-Asp-(O*t*Bu)-Lys(Boc)–Wang resin. Subsequently, the cleavage of the Fmoc group was carried out.

DIPC (16.4 mL, 0.105 mmol) was added to a solution of compound **5** (93.9 mg, 0.105 mmol) and HOBt (14.2 mg, 0.105 mmol) in dichloromethane/DMF (5:1, 500 mL) at 0 °C. The solution was stirred for 1 h under Ar. The mixture was added to the resin in a reaction vessel and shaken for 5 h. The resin was filtered and washed with DMF (1 mL, 1 min × 5) and dichloromethane (1 mL, 1 min × 5), and the reaction was checked by using the BPB test. After cleavage of the Fmoc group, the resin was washed with dichloromethane (1 mL, 1 min × 5) and dried in vacuo.

Cleavage from the resin: The dry peptide resin was treated with trifluoroacetic acid/water/1,2-ethandithiol/triisopropylsilane (9.45:0.25:0.25:0.1, *v/v/v/v*, 500 μL) for 1 h. The resin was washed with TFA solution (1 mL, 5 min × 5) and dichloromethane (1 mL, 5 min × 5) and the combined filtrates were concentrated in vacuo and lyophilized from *tert*-butyl alcohol. The residue was washed with water and methanol to give lipopeptide fragment LPSA-01 as a white solid. ESI-MS (positive) *m/z* 899.97 $[M+2H]^{2+}$, 600.32 $[M+3H]^{3+}$; ^{1}H NMR (600 MHz, [D_6]DMSO): δ = 8.70–7.55 (m, 14H; –CON*H*–, Lys-NH_2, Cys-NH_2), 7.50–6.46 (m, 8H; His-Ar*H*, Arg-N*H*, Asn-NH_2), 5.15 (m, 1H; *S*-glyceryl-OC*H*), 4.68–3.94 (m, 11H; –NH–*CH*–CO–, Ser-CH_2, Thr-C*H*), 4.34 (m, 1H; *S*-glyceryl-OCH*H*), 4.16 (m, 1H; *S*-glyceryl-OCH*H*), 3.66–3.52 (m, 4H; 2Ser-CH_2), 3.40–2.70 (m, 5H; His-CH_2, Lys-eCH_2, Asp-CH_2), 2.86 (m, 1H; *S*-glyceryl-CH*H*), 2.78 (m, 1H; *S*-glyceryl-CH*H*), 2.80–1.94 (m, 8H; Glu-CH_2, PamCH_2–COO, Arg-CH_2), 1.82–4.42 (m, 10H; Lys-bCH_2, gCH_2, dCH_2, PamCH_2–CH_2–

COO), 1.36–.1.18 (m, 54H; Ala-CH_3, Thr-CH_3, Pam-CH_2), 0.87–0.83 (t, J=7.2 Hz, Pam-CH_3).

Other lipopeptides were also synthesized in a similar way to LPSA-01. ESI-MS (positive) LPSA-02: *m/z* 1618.98 $[M+H]^+$, 809.95 $[M+2H]^{2+}$; LPSA-03: *m/z* 1604.95 $[M+H]^+$, 802.91 $[M+2H]^{2+}$; LPSA-04: *m/z* 874.02 $[M+2H]^{2+}$; LPSA-05: *m/z* 926.03 $[M+2H]^{2+}$; LPSA-06: *m/z* 1687.92 $[M+H]^+$, 844.48 $[M+2H]^{2+}$; LPSA-07: *m/z* 856.46 $[M+2H]^{2+}$; LPSA-08: *m/z* 866.44 $[M+2H]^{2+}$; LPSA-09: *m/z* 837.94 $[M+2H]^{2+}$; LPSA-10: *m/z* 852.50 $[M+2H]^{2+}$; LPSA-11: *m/z* 801.00 $[M+2H]^{2+}$; LPSA-12: *m/z* 858.53 $[M+2H]^{2+}$; LPSA-13: *m/z* 1799.16 $[M+H]^+$, 899.97 $[M+2H]^{2+}$; LPSA-07-2: *m/z* 920.54 $[M+2H]^{2+}$; LPSA-14: *m/z* 1740.56 $[M+H]^+$, 870.72 $[M+2H]^{2+}$; LPSA-14-2: *m/z* 1452.13 $[M+H]^+$, 968.38 $[M+2H]^{2+}$; Pam_2CSK_4: *m/z* 1272.16 $[M+H]^+$, 636.58 $[M+2H]^{2+}$, 424.72 $[M+3H]^{3+}$.

Luciferase assay: Ba/F3 cells stably expressing p55IgκLuc, an NF-κB DNA-binding activity dependent luciferase reporter construct (Ba/κB), murine TLR2, the p55IgκLuc reporter construct (Ba/mTLR2), murine TLR4/MD-2 and the p55IgκLuc reporter construct (Ba/mTLR4/mMD-2) were kindly provided by Prof. Kensuke Miyake (Institute of Medical Science, University of Tokyo, Japan). NF-κB-dependent luciferase activity in these cells was determined as described previously.[25]

Cytokine assay: Eight-week-old male BALB/c mice were obtained from Kyudo (Kumamoto, Japan). The animals received humane care in accordance with our institutional guidelines and the legal requirements of Japan. Stimulation of thioglycolate elicited peritoneal exudate cells (PEC), stimulation of Histopaque-separated human PBMCs from a healthy donor (M.F.), and the cytokine assay for secreted murine or human TNF-α were performed as described elsewhere.[14]

Acknowledgements

This work was supported in part by Grants-in-Aid for Scientific research from the Japan Society for the Promotion of Science (No. 19310144, 20241053), and by Osaka University G-COE program for Frontier Biomedical Science Underlying Organelle Network Biology.

Keywords: immunology · lipoproteins · *Staphylococcus aureus* · Toll-like receptor 2

[1] E. M. Creagh, L. A. O'Neill, *Trends Immunol.* **2006**, *27*, 352–357.
[2] U. Zähringer, B. Lindner, S. Inamura, H. Heine, C. Alexander, *Immunobiology* **2008**, *213*, 205–224.
[3] V. Braun, K. Rehn, *Eur. J. Biochem.* **1969**, *10*, 426–438.
[4] V. Braun, *Biochim. Biophys. Acta* **1975**, *415*, 335–377.
[5] K. Hantke, V. Braun, *Eur. J. Biochem.* **1973**, *34*, 284–296.
[6] K. H. Wiesmüller, W. Bessler, G. Jung, *Hoppe. Seylers Z. Physiol. Chem.* **1983**, *364*, 593–606.
[7] P. F. Mühlradt, H. Meyer, R. Jansen, *Biochemistry* **1996**, *35*, 7781–7786.
[8] P. F. Muhlradt, M. Kiess, H. Meyer, R. Süssmuth, G. Jung, *J. Exp. Med.* **1997**, *185*, 1951–1958.
[9] K. Tawaratsumida, M. Furuyashiki, M. Katsumoto, Y. Fujimoto, K. Fukase, Y. Suda, M. Hashimoto, *J. Biol. Chem.* **2009**, *284*, 9147–9152.
[10] K. Kurokawa, H. Lee, K.-B. Roh, M. Asanuma, Y. S. Kim, H. Nakayama, A. Shiratsuchi, Y. Choi, O. Takeuchi, H. J. Kang, N. Dohmae, Y. Nakanishi, S. Akira, K. Sekimizu, B. L. Lee, *J. Biol. Chem.* **2009**, *284*, 8406–8411.
[11] K. Shibata, A. Hasebe, T. Into, M. Yamada, T. Watanabe, *J. Immunol.* **2000**, *165*, 6538–6544.
[12] I. C. Sutcliffe, R. R. Russell, *J. Bacteriol.* **1995**, *177*, 1123–1128.
[13] H. Stoll, J. Dengjel, C. Nerz, F. Götz, *Infect. Immun.* **2005**, *73*, 2411–2423.
[14] M. Hashimoto, K. Tawaratsumida, H. Kariya, A. Kiyohara, Y. Suda, F. Krikae, T. Kirikae, F. Götz, *J. Immunol.* **2006**, *177*, 3162–3169.
[15] M. Hashimoto, K. Tawaratsumida, H. Kariya, K. Aoyama, T. Tamura, Y. Suda, *Int. Immunol.* **2006**, *18*, 355–362.
[16] M. Hashimoto, M. Furuyashiki, R. Kaseya, Y. Fukada, M. Akimaru, K. Aoyama, T. Okuno, T. Tamura, T. Kirikae, F. Kirikae, N. Eiraku, H. Morioka, Y. Fujimoto, K. Fukase, K. Takashige, Y. Moriya, S. Kusumoto, Y. Suda, *Infect. Immun.* **2007**, *75*, 1926–1932.
[17] K. Sankaran, H. C. Wu, *J. Biol. Chem.* **1994**, *269*, 19701–19706.
[18] H. Y. Qi, K. Sankaran, K. Gan, H. C. Wu, *J. Bacteriol.* **1995**, *177*, 6820–6824.
[19] M. M. Babu, M. L. Priya, A. T. Selvan, M. Madera, J. Gough, L. Aravind, K. Sankaran, *J. Bacteriol.* **2006**, *188*, 2761–2773.
[20] J. W. Metzger, K. H. Wiesmüller, G. Jung, *Int. J. Pept. Protein Res.* **1991**, *38*, 545–554.
[21] J. Metzger, G. Jung, W. G. Bessler, P. Hoffmann, M. Strecker, A. Lieberknecht, U. Schmidt, *J. Med. Chem.* **1991**, *34*, 1969–1974.
[22] P. H. G. Zarbin, A. R. M. Oliveira, F. Simonelli, J. A. F. P. Villar, O. Delay, *Tetrahedron Lett.* **2004**, *45*, 7399–7400.
[23] V. Swali, M. Matteucci, R. Elliot, M. Bradley, *Tetrahedron* **2002**, *58*, 9101–9109.
[24] DOLOP; http://www.mrc-lmb.cam.ac.uk/genomes/dolop/analysis.shtml
[25] K. Shibata, A. Hasebe, T. Sasaki, T. Watanabe, *FEMS Immunol. Med. Microbiol.* **1997**, *19*, 275–283.

Received: April 21, 2009
Published online on ■■ ■■, 2009

*Y. Fujimoto, M. Hashimoto, M. Furuyashiki, M. Katsumoto, T. Seya, Y. Suda, K. Fukase**

■■-■■

Lipopeptides from *Staphylococcus aureus* as Tlr2 Ligands: Prediction with mRNA Expression, Chemical Synthesis, and Immunostimulatory Activities

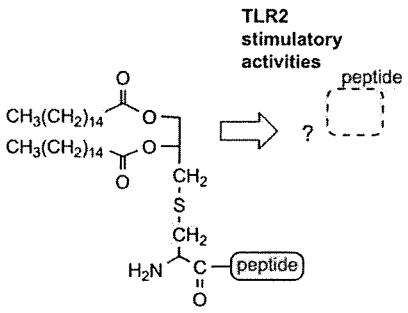

Chemically synthesized lipopeptides based on natural lipoproteins from *S. aureus*

Recognize this? Based on predictions from mRNA expression of lipoproteins from *Staphylococcus aureus*, lipopeptide fragments were chemically synthesized, and their TLR2-stimulatory activities and cytokine-induction capabilities were analyzed. All the lipopeptides activated TLR2, but the activities varied depending on their peptide sequences.

